Carbon Negative Geothermal: Techno-Economic Analysis of Geothermal Energy combined with Direct and Biomass-Based Carbon Dioxide Removal

Karan Titus[1], David Dempsey[1], Rebecca Peer[1], Rosalind Archer[2]

[1]The University of Canterbury, 20 Kirkwood Avenue, Upper Riccarton, Christchurch 8041, New Zealand

[2]Griffith University, Gold Coast Campus Parklands Drive Southport, Qld 4222, Australia

karan.titus@pg.canterbury.ac.nz

This manuscript has been submitted for publication. This version is a non-peer reviewed preprint submitted to EarthArXiv. Subsequent versions of this manuscript may change slightly different content. Please feel free to contact any of the authors.

Carbon Negative Geothermal: Techno-Economic Analysis of Geothermal Energy combined with Direct and Biomass-Based Carbon Dioxide Removal

Karan Titus[1], David Dempsey[1], Rebecca Peer[1], Rosalind Archer[2]

[1]The University of Canterbury, 20 Kirkwood Avenue, Upper Riccarton, Christchurch 8041, New Zealand

[2] Griffith University, Gold Coast Campus Parklands Drive Southport, Qld 4222, Australia

karan.titus@pg.canterbury.ac.nz

Keywords: *Geothermal, BECCS, DACCS, forestry residues, energy economics*

Abstract

Limiting global temperature rise to between 1.5 and 2°C will likely require widespread deployment of carbon dioxide removal (CDR) technologies for sectors with hard-to-abate emissions. As financial resources for decarbonization are finite, strategic deployment of CDR technologies is essential for maximizing atmospheric CO_2 reductions. Carbon capture and sequestration (CCS), using either direct air capture (DACCS) or bioenergy (BECCS) technologies has a particular synergy with geothermal energy generation. This is because it can leverage expensive geothermal infrastructure for dissolved CO_2 storage in subsurface reservoirs.

Here, we argue that the use of existing well apparatuses and a lack of offsite CO_2 transportation costs substantially improves the economic feasibility of geothermal-based CDR schemes over traditional approaches. We further argue that revenues from net-negative CO_2 emissions and increased power production should be used to lower the net costs of decarbonization activities. To test these ideas, we compared the techno-economic performance of geothermal-BECCS and geothermal-DACCS plant designs against conventional geothermal operations. We did this using a systems model that quantifies energy, carbon and financial flows through those designs.

At a CO_2 market price of $100/tonne, geothermal-BECCS was more cost effective at electricity generation ($69/MWh) than geothermal-DACCS ($143/MWh) and traditional geothermal ($81/MWh). New geothermal-BECCS plants also achieved the lowest costs of emissions abatement, $145/t$CO_2$, which includes both carbon removal and the displacement of fossil-fuel generation. Abatement costs are even lower, $41/t$CO_2$, for BECCS retrofit of existing geothermal plants due to pre-existing infrastructure (wells, steam field, plant).

Although geothermal-DACCS removes CO_2 at high rates, its high parasitic load increases the overall decarbonization cost ($197/t$CO_2$). In contrast, when biomass hybridization is considered, geothermal-BECCS produced 20% more electricity than the benchmark geothermal plant. We conclude that this increase in electricity production makes geothermal-BECCS the more cost-effective geothermal-based CDR configuration.

1. Introduction

There is a timely need for specialized and cost-effective decarbonisation solutions. The sixth annual report (AR6) from the Intergovernmental Panel on Climate Change (IPCC) states with high confidence that limiting global warming to 1.5-2°C will require net-zero CO_2 emissions by 2050 (IPCC, 2023). Even if 100% renewable electrification is achieved, hard-to-abate emissions from agriculture, aviation, shipping and industrial processes would still pose challenges for global climate targets. Therefore, the IPCC highlight deployment of carbon dioxide removal (CDR) technologies as critical to counterbalance these emissions (IPCC, 2023).

Geothermal energy is a mature, low-carbon source of baseload electricity that relies on hot fluid extracted from deep wells (Vargas et al., 2022). Traditionally, geogenic CO_2 emissions brought up with the hot fluid have been vented to atmosphere. However, recent advances in emissions capture and reinjection present new opportunities for geothermal wells to also perform a carbon sequestration function. When this CO_2 comes from the atmosphere, the result is geothermal-enabled carbon dioxide removal (CDR).

Geothermal energy has been combined with direct air carbon capture and storage (DACCS) at demonstration scale (Ratouis et al., 2022). Leveraging similar technology, Titus et al. (2023) propose that geothermal energy could also be combined with bioenergy-based carbon capture and storage (BECCS). In addition to carrying out atmospheric CDR, such a scheme would also increase renewable electricity production above a standard geothermal baseline.

Both BECCS and DACCS are important technologies in climate mitigation pathways that limit global temperature increase to 2°C (Fasihi et al., 2019; Gough et al., 2018). The extent of their synergy and financial viability with geothermal energy is currently unknown and should be robustly explored. We introduce a new configuration of geothermal-BECCS and compare its performance to a benchmark geothermal power plant and a geothermal-DACCS power plant for high-temperature geothermal reservoir. This research is novel because it is the first techno-economic comparison of geothermal-based CDR configurations with conventional geothermal plants. Furthermore, we quantify the effect and implications of intrinsic geogenic emissions and feedstock transportation distance on geothermal-based CDR activities.

Through the methodology of this study, we delineate the market conditions for which geothermal-based CDR systems is more cost-effective than conventional geothermal plants. We estimate the initial investment cost for geothermal-CDR to reach 1 $MtCO_2$/year of net negative emissions, thereby contributing to the wider conversation of decarbonisation tools and advances in geothermal energy. Our approach can be applied on a case-by-case basis for new geothermal-CDR developments to estimate their decarbonisation potential.

1.1. Geogenic CO_2 capture in geothermal systems

Geothermal power plants emit CO_2 at worldwide average rates of 122 gCO_2/kWh (Bayer et al., 2013; Bertani & Thain, 2002). This CO_2 is geogenic in nature, originating from deep magmatic intrusions – hence, sometimes referred to as magmatic emissions – and brought to the surface by the geothermal fluid (Kaya & Zarrouk, 2017). Although these emission intensities are lower than natural gas (~400 gCO_2/kWh) and coal generation (~1000 gCO_2/kWh), a global trend of geogenic CO_2 reinjection is emerging (Kaya & Zarrouk, 2017; Ratouis et al., 2022).

The practice of in-line dissolution of geogenic CO_2 into geothermal reinjection wells was pioneered during the Carbfix project in 2012 at the Hellisheidi geothermal power plant in Iceland (Sigfusson et al., 2015). The goal was to capture CO_2 and H_2S that would otherwise be vented to atmosphere from the plant's cooling system (Gunnarsson et al., 2018). Unlike traditional carbon capture & storage (CCS) operations that inject a buoyant pure CO_2 phase directly into subterranean formations, in-line dissolution dissolves the CO_2 into a dense brine prior to its injection. This is achieved using an interior pipe, bubbler and brine hydrostatic column within the reinjection well. Total storable CO_2 is thus limited by its solubility in brine, which is sensitive to pressure and, to a lesser extent, temperature and salinity (Duan & Sun, 2003).

Conventional CCS operations often require new transport and injection infrastructure, which can increase capital expenditure (CAPEX) by 45-130% and operational expenditure (OPEX) by 4-58% over a conventional fossil fuel plant (Gough et al., 2018). At Carbfix, in-line dissolution proved more economical than conventional CCS because reinjection wells were already available, CO_2 didn't need offsite transportation, and subcritical (as opposed to supercritical) compression reduced the parasitic load (Gunnarsson et al., 2018).

Although sequestration potential is capped by solubility, a key advantage of dissolving CO_2 is avoiding buoyancy-driven leakage risks (Kervévan et al., 2017). Carbonated brine is slightly denser than an equivalent non-carbonated fluid (Garcia, 2001) and is hence likely to sink towards the bottom of the reservoir. Further, CO_2 is more likely to stay dissolved if reservoir pressure is maintained (Kaya & Zarrouk, 2017), which is promoted under the standard reservoir management practice of reinjection of produced fluids. Finally, with favourable geology, subsurface chemical rock reactions can allow reinjected CO_2 to mineralise, a nigh permanent form of storage (Marieni et al., 2018; Sigfusson et al., 2015). At Carbfix, chemical tracer testing showed that 98% of the reinjected geogenic CO_2 mineralised within two years.

With in-line dissolution to sequester geogenic CO_2, geothermal resources can provide carbon-neutral energy. However, geothermal energy can also be paired with direct or biogenic CO_2 capture methods, which enables a carbon-negative energy cycle.

1.2. Geothermal with direct air carbon capture and sequestration

In 2019, global net annual anthropogenic greenhouse gas emissions reached 59±6.6 $GtCO_2$ (IPCC, 2023). To reach net zero by 2050, this could require CO_2 emissions cuts by ~ 4% each year (Lawrence et al., 2018). Direct air carbon capture and sequestration (DACCS) is one method to offset non-point source emissions at scale and aid in the global net zero effort.

For DACCS to reach a scale of 10 $GtCO_2$/year by 2050 (~17% of 2019 emissions), Breyer et al. (2019) have suggested that investments in the range €32-42 billion (~$34-45 billion) are required. This is on par with investments in solar-PV between 1996 and 2005.

DACCS can be deployed in two ways: (1) as a high-temperature (HT) aqueous solution-based process or (2) a low-temperature (LT) solid sorbent-based process. Both require electricity and heat as inputs. For example, HT-DACCS requires temperatures of about 900°C, which can be obtained from burning fossil fuels or syngas (Sabatino et al., 2021). In contrast, LT-DACCS requires temperatures of about 100°C for emissions capture, which can be obtained from separated geothermal brine (Breyer et al., 2019). Coupled with in-line dissolution for permanent disposal, geothermal-DACCS is a technically feasible CDR operation (see Figure 1A for a process schematic of geothermal-DACCS).

At the Carbfix 2 project, a pilot-scale geothermal-DACCS plant was installed in 2017. The plant captured 50 tCO_2/year for storage through in-line dissolution (Gutknecht et al., 2018; Ratouis et al., 2022). The separation process requires a substantial amount of heat (5.4-11.9 $MJ_{th}/kgCO_2$) and electricity (1.8-2.6 $MJ_e/kgCO_2$), both of which conventional geothermal power plants can provide (Fasihi et al., 2019; Sabatino et al., 2021). Separated brine at 120°C was sufficient to provide the heating load at the Carbfix 2 pilot (Gutknecht et al., 2018).

The electricity required to separate and compress CO_2 from atmospheric air is deducted from the electricity produced by the geothermal system. Thus, the economic feasibility of geothermal-DACCS is dependent on installation costs, the price of electricity and revenue from selling CO_2 offsets.

1.3. Geothermal with bioenergy & carbon capture and sequestration

Bioenergy with carbon capture and storage (BECCS) can be used to remove CO_2 from the atmosphere. Because biomass absorbs CO_2 directly from the atmosphere during its life cycle, combining bioenergy with CCS results in a net carbon-negative process (Gough et al., 2018).

The main advantage of BECCS is the coproduction of renewable electricity with CDR. The global potential for bioenergy is estimated to be 50-300 EJ/year and the potential for biogenic CDR is 2-10 GtCO_2/year by 2050 (Gough et al., 2018). This dual-decarbonisation effect is unique among other CDR technologies and BECCS was cited as a resilient power system by the IPCC (IPCC, 2023). However, for BECCS to be an effective decarbonisation tool, the net CDR of the cycle must factor in supply chain emissions, land-use emissions and storage-related losses (Gough et al., 2018).

In-line dissolution could theoretically be used to permanently dispose of biogenic CO_2 emissions captured from geothermal-biomass hybrids (Titus et al., 2023). Unlike direct capture, BECCS has the potential to increase renewable electricity production from a geothermal power plant. Therefore, it is valuable to investigate geothermal-BECCS as a means to feasibly increase electricity generation from geothermal resources

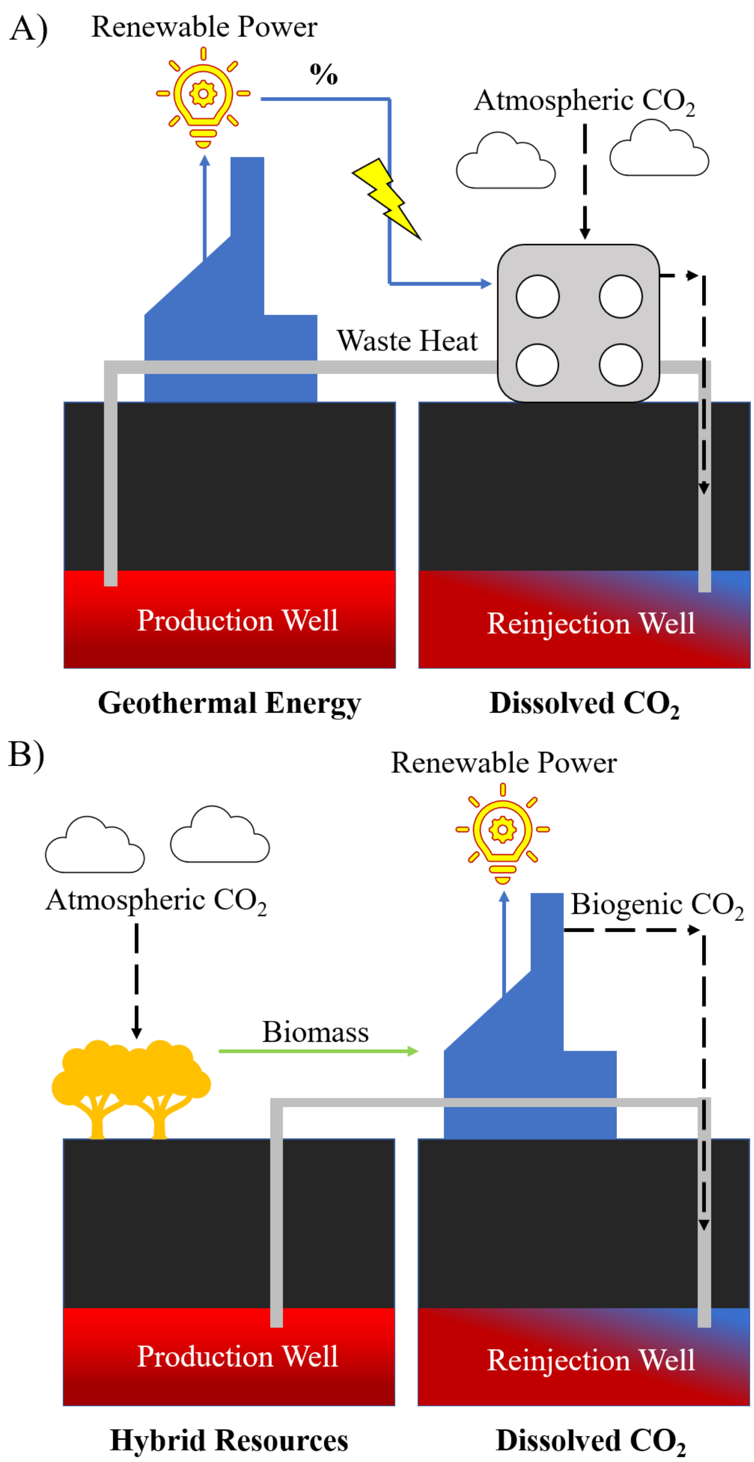

Figure 1: Process schematic of (A) geothermal-DACCS and (B) geothermal-BECCS. For (A): geothermal fluid is produced and flashed for electricity in the power plant. A percentage of that electricity, and heat from the separated brine, is used to separate CO_2 from the atmosphere in a direct air capture unit. The CO_2 is dissolved in the brine within the reinjection column and sequestered in the geothermal reservoir. For (B): geothermal fluid heat is augmented by combustion of biomass for electricity production. The resultant biogenic CO_2 is dissolved in the brine within the reinjection

Geothermal-biomass hybridisation already exists for flash (Dal Porto et al., 2016) and binary plants (Toselli et al., 2019) to enhance renewable electricity production. Titus et al. (2023)

suggested that biogenic CO_2 from geothermal-biomass hybrids could be sequestered through in-line dissolution to create a negative emissions cycle with increased renewable power (Fig. 1B).

To avoid the accumulation of nitrogen gas caps in the reinjection zone, biogenic CO_2 must be produced at a sufficiently high purity (>80%) prior to dissolution in the geothermal brine (Galiègue & Laude, 2017). This requires post-combustion capture of CO_2 from biogenic flue gas, which is investigated in this study with oxy-fuel combustion (or oxy-combustion). This post-combustion capture technique combusts feedstock in pure oxygen rather than air, resulting in a flue gas composed of 90-99% CO_2 (Zhou et al., 2016). The O_2 input is most commonly produced through cryogenic distillation of air in an air separation unit (ASU), which incurs a specific parasitic load of 184-260 kWh per tonne of O_2 (Hanak et al., 2017).

The CO_2 compression unit (CPU) also incurs a parasitic load, 90-170 kWh/tCO_2, though the lower required pressure for in-line dissolution (~50 bar) versus supercritical storage (>73.8 bar) elicits less of a penalty. Therefore, the increased power through hybridisation must exceed the parasitic load of air separation and CO_2 compression if there is to be a net increase in electricity dispatch.

Unlike direct capture, geothermal-BECCS is reliant on feedstock colocation and supply chain stability, which could limit the plant's flexibility. Land-use competition with food production is another concern, shared by all potential biomass-based climate change solutions (Sandalow et al., 2021).

1.4. Financial indicators for the co-production of electricity and carbon dioxide removal

One of the key financial indicators used to compare electricity generation technologies is the levelised cost of electricity (LCOE; IRENA 2021). Accounting for the time value of money, LCOE quantifies the net present value of the cost per unit of electricity generated over the lifetime of a given power plant. LCOE accounts for all CAPEX, future OPEX and fuel costs. For a project to be profitable, LCOE should be less than the price that electricity can be sold in a given market.

Conventional geothermal energy developments typically incur high CAPEX, low OPEX and zero fuel costs (Dickson & Fanelli, 2013). In contrast, bioenergy for electricity generation is dependent on low cost feedstocks to reach cost-competitiveness (IRENA, 2021).

In 2021, geothermal and bioenergy power plants had global weighted LCOE averages of \$68/MWh and \$67/MWh, respectively (IRENA, 2021). In the same year, new bioenergy plants had lower global average CAPEX rates (\$2,353/kWe) compared to geothermal plants (\$3,991/kW).

Power plants with concurrent electricity generation and CDR incur generally higher costs (Yang et al., 2021; Zang et al., 2020). To balance this, the net present revenue from CO_2 removal is deducted from the net present costs on a per unit of electricity generation basis. Thus, if a project is to avoid an LCOE penalty, the market price of sequestered CO_2 must be high enough to offset the increased costs. For example, for geothermal-BECCS, revenue from increased renewable electricity and CDR comes at the cost of fuel and flue-gas purification. In contrast, for geothermal-DACCS, additional investment costs for CDR and subsequent parasitic loads must be offset by the revenue from CO_2 sequestration.

An acceptable LCOE will largely depend on local market conditions and grid makeup. LCOE values from BECCS case studies (supercritical CO_2 storage) range from \$78 to 270/MWh

(Table 1), which is higher than conventional biomass plants ($67/MWh). This indicates a disincentive for CDR to be pursued alongside electricity generation.

Table 1: Levelised cost of electricity for different electricity producers by case study

Conventional Generators (Global Weighted Average, 2021)	**LCOE ($/MWh)**	
Biomass (without CCS)	67	IRENA (2021)
Geothermal energy (without CDR)	68	IRENA (2021)
BECCS Case Studies	**LCOE ($/MWh)**	
Gasification with amine-based CCS	78	Dinca et al. (2018)
Gasification combined cycle	201.2 - 273.6	Zang et al. (2020)
Oxy-gasification with staged oxy-combustion combined cycle	22.9	Khallaghi et al. (2021)
Pulverised biomass with CCS	168.6	Yang et al. (2021)
Gasification combined cycle *	228.2	Emenike et al. (2020)
Post-combustion capture*	239.8	Emenike et al. (2020)
Oxy-fuel combustion*	269.3	Emenike et al. (2020)

*Only results for wood displayed

An analogous metric to LCOE is the levelized cost of sequestration (LCOS), which quantifies the net present value of all costs per unit of CO_2 sequestered in $/t$CO_2$ over the life cycle of the plant (Lehtveer & Emanuelsson, 2021). Here, the net present revenue from electricity generation is deducted from costs. This means that sequestration through BECCS and DACCS would be sensitive to the market price of electricity. However, several complexities such as cyclical operation, start-up time and dynamic shifts in grid dispatch are difficult to represent using this metric (Lehtveer & Emanuelsson, 2021). The LCOS values of different DACCS case studies are provided in Table 2. LCOS values above $200/t$CO_2$ are generally considered uneconomic (Fasihi et al., 2019).

Table 2: Levelised cost of sequestration for different negative CO_2 emissions case studies

DACCS	**LCOS ($/t$CO_2$)**	
HT System	180 - 300	Lehtveer & Emanuelsson (2021)
LT System	200 - 350	Lehtveer & Emanuelsson (2021)

HT (Carbon Engineering)	97 - 232	Kieth et al. (2018)
Alkali Scrubbing	600	Sabatino et al. (2021)
Monoethanolamine	1690	Kiani et al. (2020)
BECCS	**LCOS (\$/tCO_2)**	
Standalone	≤ 100	Lehtveer & Emanuelsson (2021)
Biochar	46-518	Cheng et al. (2021)

LCOE and LCOS are useful metrics to assess, respectively, the electricity generation and CDR aspects of BECCS and DACCS. However, neither metric provides a complete picture of the combined decarbonisation effect on the system. The levelised cost of carbon abatement (LCCA; Friedmann et al., 2020) assesses total decarbonisation achieved through substitution of technologies that perform the same function. This metric expresses the net present value of all costs against the total displaced CO_2 emissions achieved by transitioning from a 'business as usual' (BAU, defined as current practices) to a new technology. Selecting the appropriate 'business as usual' technology is important when considering displacement, and this will vary by sector, region and frame of analysis. A list of LCCA values for low-carbon technologies is provided in Table 3.

Table 3: Levelised cost of carbon abatement per low-carbon technology type (Friedmann et al., 2020)

Low Carbon Technology	Displacing	LCCA (\$/tCO_2)
Sustainable aviation fuels	Standard aviation fuel	209-1618
Utility solar PV	California grid (2018)	91
Rooftop solar	California grid (2018)	287
Low-carbon steel alternatives (H_2, zero-CO_2 electricity, etc.)	Primary steel production	14-440
Generic electric vehicle	Fossil-based vehicle	734
Direct air carbon capture and storage	Standard aviation fuel	124-325

As global decarbonisation budgets are finite, financial indicators are essential when deciding whether to invest in BECCS or DACCS at a given geothermal resource. To address this challenge, we have developed a techno-economic systems model that can estimate key thermodynamic (net power, annual sequestration, emissions intensity) and financial indicators (LCOE, LCOS and LCCA) for geothermal-based CDR configurations.

To verify that the major processes of these CDR configurations truly achieve net negative emissions, we also calculate net emissions intensity (EI). EI is a useful metric for carbon accounting, denoted in gCO_2 emitted per unit electricity (kWh). EI is often used to compare the decarbonisation effect of low-carbon electricity generation cycles to traditional fossil fuel plants at scale.

For example, in Table 4, the BECCS configuration designed by Khallaghi et al. (2021) could remove 1.85 times the amount of CO_2 released to the atmosphere by an equivalent-sized natural gas plant. In the context of geothermal-based CDR, it can be used to determine (1) whether the specified operation is net-carbon negative, and (2) the plant size required to achieve CDR targets.

Table 4: Emissions intensity values for different electricity producers

Electricity Producer	Emissions Intensity (gCO_2/kWh)	
Coal	1012	EIA (2021)
Petroleum	966	EIA (2021)
Natural Gas	413	EIA (2021)
Geothermal (Türkiye)*	1063	Aksoy (2014)
Geothermal (Worldwide)	122	Bertani & Thain (2002)
BECCS (oxy-gasification)	-766	Khallaghi et al. (2021)
BECCS (pulverised feedstock)	-1260	Yang et al. (2021)
Geothermal-BECCS	-131 to -922	Titus et al. (2023)

*Weighted average of power plants where CO_2 is not used for commercial purposes

2. Methods

This study extends the Titus et al. (2023) thermodynamic systems model for geothermal-BECCS to include energy and mass balances relevant to geothermal-DACCS. It also adds new financial performance calculations. With this new model, we compare and assess two hybrid geothermal-CDR energy cycles against conventional geothermal and natural gas-based generation. The following sections outline the model assumptions, inputs, and configurations.

2.1 Geothermal-CDR thermodynamic and sequestration model

The Titus et al. (2023) thermodynamic model for geothermal-BECCS used mass and energy conservation to track the state of a geofluid control volume as it transited key geothermal plant apparatus. In brief, the model calculates:

1. For geothermal fluid at specified reservoir temperature and pressure, when it passes through a separator that reduces its pressure, the mass fractions of steam and brine that exit;
2. For a biomass boiler and heat exchanger installed on the geothermal steam line, the energy imparted to the steam at a given biomass burn rate;
3. For a given biomass feedstock, the resultant biogenic CO_2 emissions available for in-line dissolution, and the associated separation and compression parasitic loads;
4. For steam dispatched to the turbine, the electrical power produced for given condenser exhaust pressure;
5. For brine and condensate dispatched to a reinjection well, the maximum dissolvable CO_2 based on its temperature and downhole pressure conditions.

Thus, with reservoir temperature, geothermal production well mass rate and turbine design temperature, it is possible to compute the net electrical power generated, rate of biomass fuel consumption, and the rate of CO_2 removed via in-line dissolution. The emissions intensity of the plant (EI), which is the ratio of emissions to energy production on a gCO_2/kWh basis, is also calculated.

In this study, we extended the Titus et al. (2023) model to consider geothermal-DACCS. We did this by calculating the dissolution capacity of CO_2 at an optimal pressure <50 bar, then determining if the thermal energy available from the separated brine was sufficient to split that much CO_2 from ambient air. The amount of CO_2 that can be separated from air (and needs to be dissolved) is given by the heat requirement load (11.9 MJ_{th} per kg of CO_2, Sabatino et al., 2021).

All cost, revenue, electricity and emissions terms are represented as net present value and discounted over the plant's life (30 years) at a discount rate of 8%. We chose this discount rate because it is slightly more conservative than the value used for OECD countries (7.5%) by the International Renewable Energy Agency (IRENA, 2019; Park et al., 2021). All currency values are expressed in US dollars ($) unless otherwise stated.

2.2 Geothermal-CDR financial model

The most common economic metric to assess different electricity generation technologies is the levelised cost of electricity ($LCOE$) presented in $/MWh (IRENA, 2021):

$$LCOE = \frac{C}{G} \qquad (1)$$

where C represents all costs ($) and G represents all electricity generated (MWh). The key costs included in the numerator of Eq. (1) are CAPEX, OPEX and any relevant fuel costs. In the case of geothermal power plants, costs may also need to account for geogenic CO_2 emissions given local policy measures (Ratouis et al., 2022).

When geothermal is coupled with CDR, any revenue from CO_2 sequestered can be deducted from costs:

$$LCOE = \frac{C - R_{CO_2}}{G} \quad (2)$$

where R_{CO_2} is the CDR revenue ($). The total cost term, C, is now modified to include the new infrastructure and operational expenses associated with CDR. Furthermore, the numerator is now sensitive to the market price of CO_2. For a geothermal field with a constant mass production, the generation term G may increase (hybrid power boosting) or decrease (overall parasitic load) for a geothermal-based CDR configuration when compared to a conventional geothermal power plant.

The levelised cost of sequestration (LCOS) assesses the cost-effectiveness of sequestering CO_2 on a per-tonne basis:

$$LCOS = \frac{C - R_g}{E} \quad (3)$$

Here, the revenue from electricity production (R_g), in US dollars ($), is deducted from costs in the numerator. Net carbon removed from the atmosphere, E, is given in tCO_2. The LCOS of geothermal-BECCS and geothermal-DACCS is thus sensitive to the market price of electricity.

The levelized cost of carbon abatement (LCCA; Friedmann et al., 2020) quantifies the full decarbonisation effect of a technology:

$$LCCA = \frac{C_1}{E_0 - E_1} \quad (4)$$

As with Eqs. (2) and (3), the net present value of all costs is included in the numerator. However, instead of deducting revenue from either electricity generation or CDR, the total decarbonisation effect is represented in the denominator. E_0 is the net present value of CO_2 emissions of a 'business as usual' (BAU) technology that requires abatement (e.g., coal, natural gas, etc.). A natural gas turbine cycle has been selected as the 'business as usual' case for comparison with the geothermal configurations explored here.

E_1 is the net present value of CO_2 emissions of a low-carbon alternative such as solar-PV or geothermal energy. For net carbon-negative cycles like geothermal-BECCS and geothermal-DACCS, E_1 is a negative value and the denominator can be quite large (theoretically, unbounded). In comparison, the LCCA of carbon-neutral technologies is bounded by the emissions of the BAU technology. We assume that the price of transport emissions is already factored in the feedstock transport costs and are not double counted in Eqs. (2)-(4).Both terms in the denominator are given in tonnes of CO_2 and scaled for equivalent-sized electricity output.

The emissions intensity (EI) of geothermal-BECCS and geothermal-DACCS plants has three main contributions: (i) geogenic CO_2 that is not captured and reinjected, E_{geo}, (ii) transportation emissions associated with fuel, E_{tran}, and (iii) negative emissions from CDR, E_{CDR}. For this study, EI is calculated using Eq. (5):

$$EI = \frac{E_{geo} + E_{tran} - E_{CDR}}{G} \quad (5)$$

A limitation of EI as a metric for CDR technologies is that it doesn't convey the additional decarbonisation benefits from increasing renewable power. Nor have we included lifecycle emission from construction or land-use changes considered when practically implementing a power plant (Pehl et al., 2017). Coproduction of electricity and CDR is subject to the capacity factor of the plant typically 90% for geothermal powerplants (IRENA, 2021).

2.3 Geothermal-CDR model assumptions

Three geothermal plant configurations have been considered in this study: (1) a benchmark geothermal plant without carbon removal, (2) a geothermal-BECCS plant where separated steam is superheated with biomass before turbine expansion, and (3) a geothermal-DACCS plant where separated brine provides the heat for LT solid sorbent-based separation. All configurations were modelled as new plants, entering the electricity grid specifically to displace natural gas generation.

The three configurations share the same initial geothermal fluid production mass rate of 100 kg/s, initial reservoir temperature of 275°C, and initial reservoir pressure of 69 bar (approximately 10 bar above saturation pressure) to represent two-phase flow within the production wells. These reservoir conditions are representative of high-temperature geothermal systems such as Hellisheidi in Iceland (Lugaizi, 2011), Ngatamariki in New Zealand (Boseley et al., 2010), and the Salton Sea geothermal field (Allis et al., 2011). Condensers were set to 46.85°C to induce a vacuum (DiPippo, 2016), with water selected as the cooling medium.

Different geothermal systems have different geogenic EI values. Therefore, we tested values from zero to 1000 gCO_2/kWh (i.e., average EI from Türkiye (Aksoy, 2014)), to represent the global diversity of geothermal fields.

The Roosevelt Hot Springs (USA) hybrid geothermal-fossil plant case study was economically feasible with a feedstock transport distance of 160 km (Anno et al., 1977). Thus, for this study we tested a range of feedstock transport distance up to ten times that amount, from 0 to1600 km. A distance of 0 km would represent a biomass resource adjacent to the geothermal plant. The upper bound (1600 km) represents the length of New Zealand and would be inclusive of the length of the United Kingdom (1000 km) and California (1220 km), being a sufficiently large maximum distance for truck-based freight.

We use reference values of transport distance (80 km) and geogenic EI (75gCO_2/kWh) as representative of an average geothermal field in New Zealand's Taupo Volcanic Zone (McLean et al., 2020) in proximity to the Kaingaroa forest, an area in the world that had previously been a case study for geothermal-biomass hybrids (Thain & DiPippo, 2015).

Where relevant, isopentane was selected as the working fluid for organic Rankine cycles (ORC), and its properties were adopted from Reynolds (1979). ORC cycles are designed to operate at subcritical conditions to avoid excess heat in the binary turbine exhaust due to isopentane's retrograde nature.

Reasonable financial parameters for geothermal energy, bioenergy, oxy-combustion apparatus and direct air capture units are provided with literature sources in Table 5. For a first order of comparison, the reference prices of CO_2, feedstock and electricity were set to \$100/tCO_2, \$88/t and \$60/MWh, respectively. For all three of these parameters, sensitivity analysis was conducted with the results discussed in Section 4.

Table 5: Key model assumptions for all configurations. ASU=Air Separation Unit, CPU=CO_2 Compression Unit.

Parameters	Values	
Produced geothermal fluid rate (kg/s)	100	Assumed
Reservoir temperature (°C)	275	Lugaizi (2011)
Reservoir pressure (bar)	69	Assumed

Brine injection temperature (°C)	95	Addison et al. (2015)
Condenser temperature (°C)	46.85	DiPippo (2016)
Biogenic CO_2 emissions factor (kg/kg-wood)	1.6	Puettmann et al. (2020)
Biomass heating value (kJ/kg)	16000	Thain & DiPippo (2015)
Transport emissions factor (gCO_2/tonne-km)	105	MfE (2022)
Operation start (year)	2	Assumed
Plant life (year)	30	Assumed
Discount rate (%)	8	Assumed
Plant capacity factor (%)	90	IRENA (2021)
Geothermal CAPEX ($/kWe)	3991	IRENA (2021)
Geothermal OPEX ($/kWe/year)	115	IRENA (2021)
Biomass boiler CAPEX ($/kWe)	2353	IRENA (2021)
Biomass boiler OPEX (%CAPEX/year)	6	IRENA (2021)
ASU CAPEX ($/kWe)	185.5	Khallaghi et al., (2021)
CPU CAPEX ($/kWe)	200.4	Khallaghi et al., (2021)
ASU + CPU OPEX (%CAPEX/year)	3	Khallaghi et al., (2021)
ASU load (kWh/tO_2)	184	Hanak et al. (2017)
CPU load (kWh/tCO_2)	100	Hanak et al. (2017)
O_2 requirement (tO_2/kWe/year)	12.15	García-Luna et al. (2022)
DACCS electricity load ($MJ_{el}/kgCO_2$)	2.6	Sabatino et al. (2021)
DACCS heat load ($MJ_{th}/kgCO_2$)	11.9	Sabatino et al. (2021)
DACCS CAPEX (USD/tCO_2)	788.4	Fasihi et al. (2019)
DACCS OPEX (%CAPEX)	4	Fasihi et al. (2019)
Natural gas generation EI (gCO_2/kWh)	400	EIA (2021)
Reference price of CO_2 ($/tonne)	100	Assumed
Reference price of feedstock ($/tonne)	88	MPI (2020)
Reference price of electricity ($/MWh)	60	Keith et al. (2018)

Additional sensitivity analysis was performed to assess the impact of feedstock transport distance and base geogenic EI. Both factors are potentially prohibitive to geothermal-CDR if they are large enough that negative CO_2 emissions are precluded.

Biogenic CO_2 emissions from the combustion of forestry residues range from 0.78-3.25 kg/kg of feedstock depending on state and quality (Puettmann et al., 2020). For this study, we assumed clean ground pulpwood as the feedstock with an emissions factor of 1.6 kg/kg-wood.

The amount of biogenic CO_2 or atmospheric CO_2 produced by geothermal-BECCS and geothermal-DACCS is respectively based on the biomass burn rate and the separated brine heat. Because the CDR capacity of geothermal brine is a function of pressure and mass flow rate, it is theoretically possible that the amount of CO_2 produced by an operation could surpass the capture limit (Titus et al., 2023).

We chose a 50 bar dissolution limit that is below the critical point of CO_2 (73.8 bar). For reinjection of 74 kg/s of separated geothermal brine at and 95°C, this corresponds to a maximum sequestration rate for dissolved CO_2 of 1.59 kg/s (~50 kt/year). Beyond this threshold, CO_2 must be vented to the atmosphere as carbon-neutral emissions. Dissolution of CO_2 is only permitted in reinjection wells where the geothermal fluid has not been exposed to air to avoid the potential for oxygen corrosion (Bonafin et al., 2019).

Net negative CO_2 emissions are assumed to be a source of revenue while net positive CO_2 emissions to the atmosphere are considered a cost, priced at the same market value. This study weighs renewable electricity generation and CDR as equally valuable products to the hypothetical market. Thus, they are co-produced simultaneously during the plant's operational period (90% capacity factor). However, this may not always be the case and is discussed further in subsection 4.3. All currency values are expressed in US dollars ($).

3. Results

3.1 Model Configurations

3.1.1. Configuration 1: benchmark geothermal plant

In this configuration, the geothermal fluid (100 kg/s) is flashed in a standard vertical separator (Fig. 2). Using the optimal separator temperature method (DiPippo, 2016), the separator (S) temperature is calculated as 161°C (6.3 bar). Separated steam (26 kg/s, 2758 kJ/kg) is sent to the steam turbine (ST) and condensed to 46.85°C (~0.1 bar) in cooling system 1 (CS1) before being reinjected via injection well 2 (IW2). Cooling system 1 is assumed to be a direct contact condenser with a natural draught cooling tower, with readily available water as the cooling medium. We assume that geogenic CO_2 vents from the plant through cooling system 1, rather than being recaptured.

Because the separated brine (74 kg/s) still retains a lot of energy, it is suitable to provide heat for a subcritical ORC cycle. The working fluid is assumed to be isopentane and the binary turbine (BT) inlet pressure is set to the separator pressure of 6.3 bar (94°C, 652 kJ/kg for saturated vapour isopentane). The isopentane is condensed to liquid at 46.85°C (0.187 bar) in a shell-and-tube condenser via cooling water in cooling system 2 (CS2). A surface pump (P) is used to compress the isopentane from 0.187 bar (249.5 kJ/kg) to 6.3 bar (250.5 kJ/kg) at 1 kWe/kg.

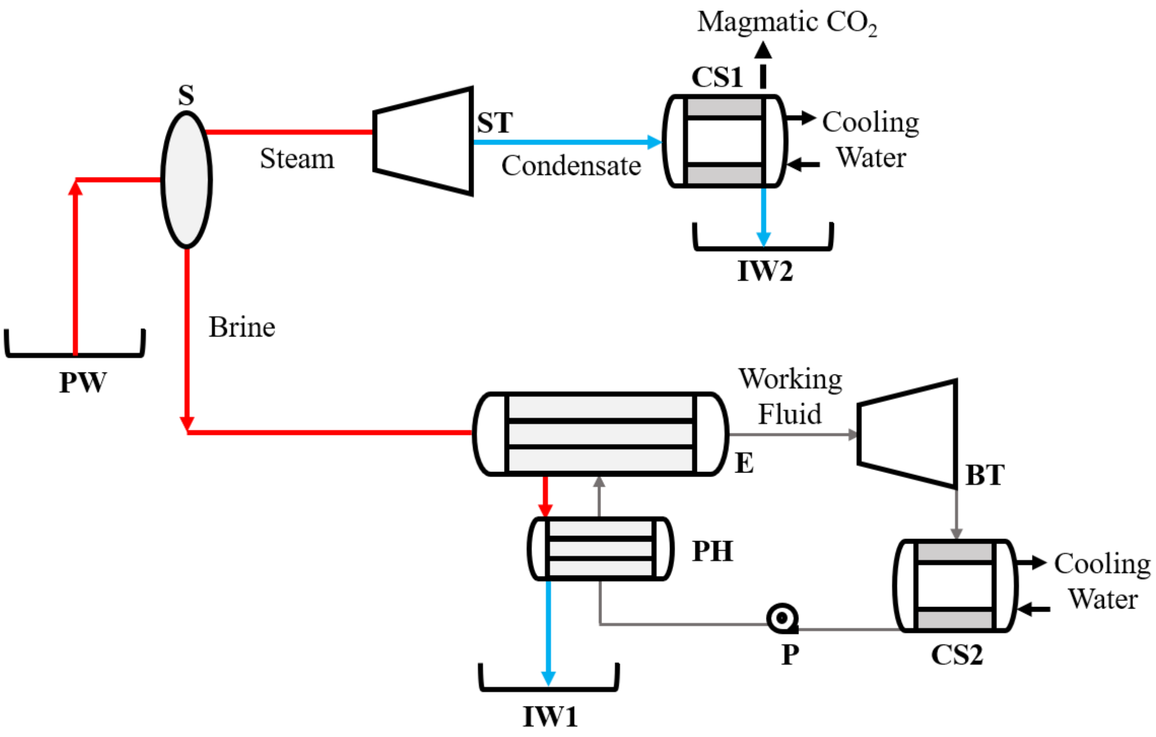

Figure 2: Schematic of a benchmark geothermal plant (Configuration 1). Individual component list follows with example values from text in brackets. PW = production well (100 kg/s), S = separator (6.3 bar), ST = steam turbine (11.9 MWe), BT = binary turbine (1.87 MWe), E = evaporator (exits at 652 kJ/kg), PH = preheater (enters at 249.5 kJ/kg), P = Pump (1 kWe/kg), CS1 = cooling system 1 (46.85°C), CS2 = cooling system 2 (46.85°C), IW1 = injection well 1 (95°C, 74 kg/s), IW2 = injection well 2 (46.85°C, 26 kg/s). Red line = hot geothermal fluid, blue line = cold geothermal fluid, grey line = isopentane, black-dashed line = CO_2. Plant not to scale.

The evaporator (E) and preheater (PH) are modelled as a single thermodynamic unit, with the brine exit temperature set to a typical dispatch temperature of 95°C (Addison et al. 2015). The mass flow of isopentane is ~51 kg/s and the total thermal energy imparted by the brine is 20.4 MW_{th}.

The work done by the steam turbine and binary turbine is 11.9 MWe and 1.87 MWe, respectively (including dry steam and generator efficiency, see Appendix A). After deducting the surface pump work (0.051 MWe), the net power produced by the plant is 13.7 MWe. The geogenic emissions are 8.1 $ktCO_2$/yr. The CAPEX and OPEX of the plant are calculated using the respective rates for geothermal power plants (net power) in Table 5.

3.1.2. Configuration 2: geothermal-BECCS plant

This configuration modifies the base geothermal plant with a biomass superheater (BIO) in the steam line between the separator and turbine (Fig. 3). The binary cycle power output and geogenic emissions are the same as the benchmark plant.

Forestry waste is used to superheat separated steam from 161°C (2758 kJ/kg) to 370°C (3207 kJ/kg), a reasonable limit when considering the mineral and corrosive elements in geothermal fluid (Dal Porto et al., 2016). This was the same temperature limit designed at the Cornia-2 geothermal-biomass hybrid plant in Larderello, Italy. With 26 kg/s of superheated steam, biomass is burned at a rate of 0.9 kg/s for forestry residues with a heating value of 16 000 kJ/kg and 25% moisture content (Thain & DiPippo, 2015). The output of the steam turbine (ST) in the hybrid plant is 18.2 MWe, an increase of 6.3 MWe over the base geothermal plant.

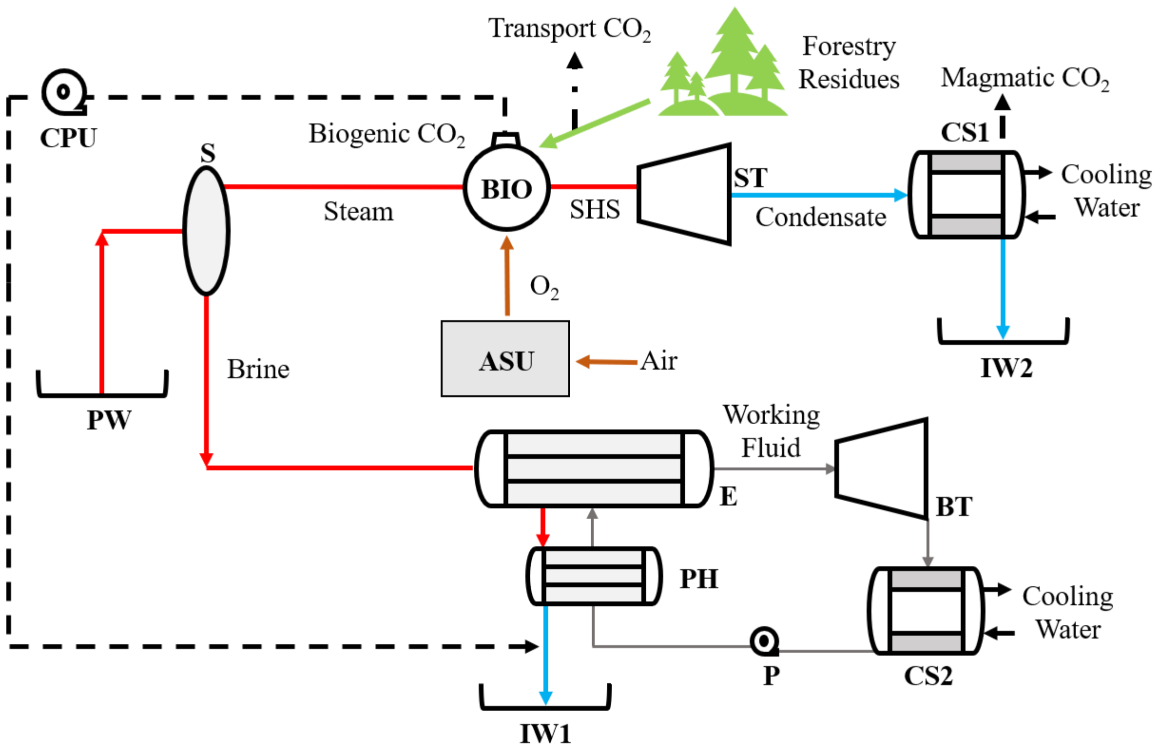

Figure 3: Schematic of a geothermal-BECCS plant (Configuration 2). Individual component list follows with example values from text in brackets. PW = production well (100 kg/s), S = separator (6.3 bar), ST = steam turbine (18.2 Mwe), BT = binary turbine (1.87 Mwe), E = evaporator (exits at 652 kJ/kg), PH = preheater (enters at 249.5 kJ/kg), P = Pump (1 kWe/kg), CS1 = cooling system 1 (46.85°C), CS2 = cooling system 2 (46.85°C), IW1 = injection well 1 (95°C), IW2 = injection well 2 (46.85°C). BIO = biomass superheater (0.9 kg/s), ASU = air separation unit (1170 kWe), CPU = compression unit (488 kWe). Red line = hot geothermal fluid, blue line = cold geothermal fluid, grey line = isopentane, black-dashed line = CO_2, green line = biomass feedstock, orange line = external atmospheric gas. Plant not to scale.

The biogenic CO_2 emissions factor of the forestry residues is 1.6 kg/kg-wood (Puettmann, 2020). The mass flow rate of the biogenic CO_2 is thus 1.4 kg/s.

An air separation unit (ASU) is used to separate oxygen from air for oxy-combustion. The ASU electricity load is 184 kWh/tO_2. We assume the oxygen required for an oxy-combustion-based BECCS plant is 12.2 t/kWe/year (García-Luna et al., 2022). For geothermal-BECCS, this applies only to the difference in steam turbine (ST) work between the hybrid plant (18 200 kWe) and the original plant (11 900 kWe), translating to an O_2 requirement of 1.74 kg/s.

The biogenic CO_2 can only be sequestered via injection well 1 (IW1) because the separated brine has not come into contact with oxygen. As a result, only 74 kg/s of the original 100 kg/s is suitable for dissolution capacity. The minimum pressure to dissolve 1.4 kg/s of CO_2 in 74 kg/s of geofluid is ~44 bar (Duan & Sun, 2003). Gross biogenic emissions sequestration is therefore 40.6 ktCO_2/yr.

The transport emissions factor of freight is 105 gCO_2/tonne-km (MfE, 2022), resulting in annual emissions from transport of forestry waste of 0.21 $ktCO_2$/year, which is only 0.5% of biogenic sequestration. At the maximum considered range of 1600 km, this would increase to 4.3 $ktCO_2$/year or about 10% of biogenic sequestration.

A compression unit (CPU) is used to compress biogenic CO_2 to 44 bar, requiring 488 kWe. The total power required for the ASU is 1170 kWe. Thus, the net power of this configuration is 16.5 MWe, a 20% increase over the base geothermal plant. After deducting transport and geogenic emissions, the net CDR of the plant is 32.3 $ktCO_2$/year. This means that the geothermal-BECCS plant provides carbon removal at roughly four times the rate that the benchmark geothermal plant is carbon emitting. To achieve this, 25.4 kt/year of forestry residues are required.

The CAPEX and OPEX of geothermal apparatuses remain the same from the base plant. The CAPEX and OPEX for the superheater, ASU and CPU are calculated by multiplying the rates provided in Table 5 with the difference in power produced by the steam turbine in the hybrid plant and the original plant.

3.1.3. Configuration 3: Geothermal-DACCS plant

For this configuration, the separated brine is used to provide heat for a direct air capture unit rather than a binary cycle (Fig. 4). The same amount of thermal energy is provided (20.4 MW_{th}), resulting in the same brine reinjection temperature of 95°C at injection well 1 (IW1). Using conservative estimates, the heat load rate to separate CO_2 from atmospheric air is 11.9 $MJ_{th}/kgCO_2$ (Sabatino et al., 2021). Thus, a maximum of ~1.56 kg/s of atmospheric CO_2 can be separated with the available thermal energy from separated geothermal brine.

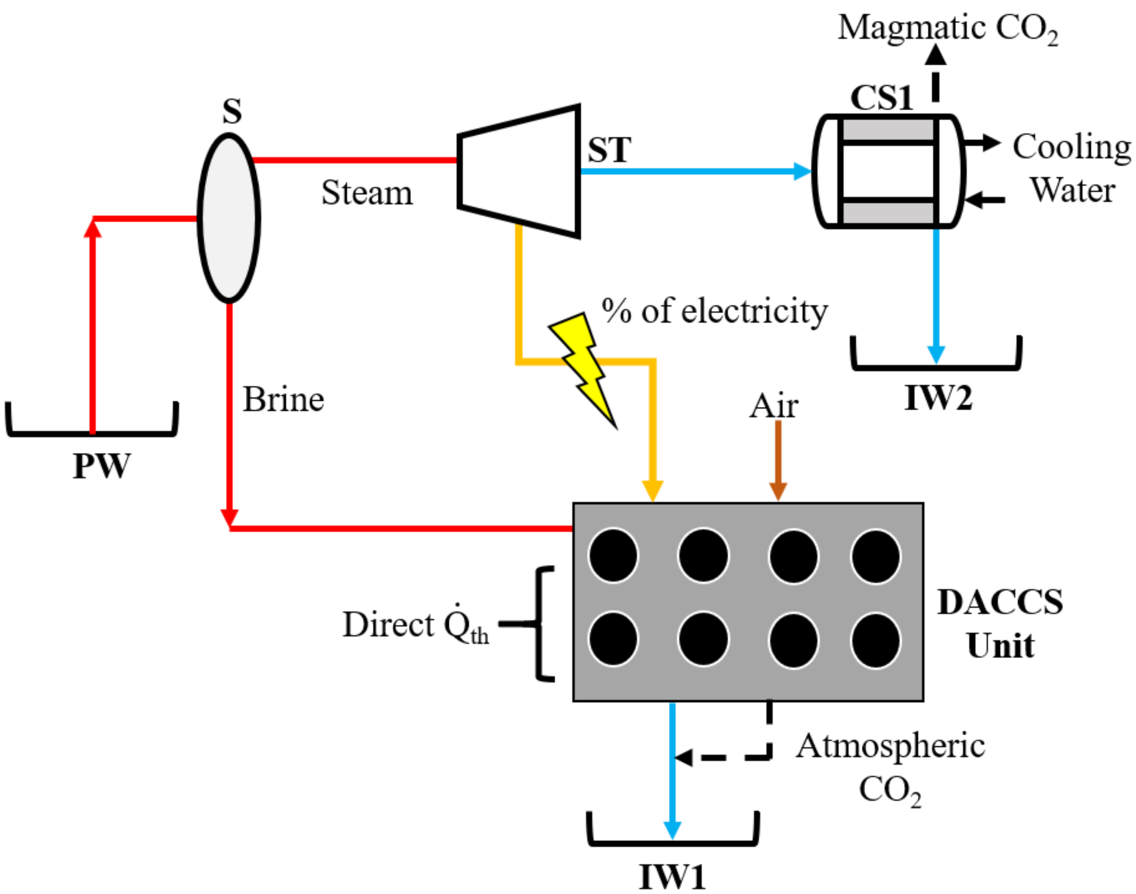

Figure 4: Schematic of a geothermal-DACCS plant (Configuration 3). Individual component list follows with example values from text in brackets. PW = production well (100 kg/s), S = separator (6.3 bar), ST = steam turbine (11.9 MWe), CS1 = cooling system 1 (46.85°C), CS2 = cooling system 2 (46.85°C), IW1 = injection well 1 (95°C), IW2 = injection well 2 (46.85°C). DACCS Unit = direct air capture unit (requires 30% of electricity produced (4 MWe) and direct heat ($\dot{Q}$th) at 20.4 MWth) . Red line = hot geothermal fluid, blue line = cold geothermal fluid, grey line = isopentane, black-dashed line = CO_2, orange line = external gas, yellow line = electricity. Plant not to scale.

Electricity is also required for the CO_2 separation process at a rate of 2.6 $MJ_{el}/kgCO_2$. This results in a parasitic load of approximately 4 MWe. The separated steam enters the steam turbine (ST) at the same conditions as the benchmark plant (161°C, 6.3 bar, 2758 kJ/kg) and produces the same gross power of 11.9 MWe. Factoring in the parasitic load required for the DACCS unit, the net power of the plant is 7.8 MWe, which is 57% of the power produced by the base geothermal plant.

Assuming a 90% capacity factor, 1.56 kg/s of atmospheric CO_2 captured equates to 49.1 tCO_2/year, an equivalent of requiring 1000 of the collectors used at Carbfix 2 (Gutknecht et al., 2018). The minimum dissolution pressure to accommodate this rate is 48.6 bar. Geogenic emissions are the same as the benchmark plant (8.1 $ktCO_2$/year) and therefore net CDR is 41 $ktCO_2$/year. This is about 30% higher than the geothermal-BECCS configuration.

The geothermal CAPEX and OPEX are now estimated using only the work done by the steam turbine. In practical cases, each key plant component would be sized for specific site conditions and the cost of materials and operation could be more appropriately determined. The CAPEX and OPEX of DACCS are calculated using the rates provided in Table 4. Model results for CAPEX, LCOE, LCOS, LCCA and EI are presented in Table 6.

3.2 Financial performance of electricity generation and carbon removal via geothermal-CDR

As shown in Table 6, a geothermal reservoir producing 100 kg/s of geothermal fluid at 275°C would yield 13.7 MWe for a conventional geothermal plant (Configuration 1), 16.5 MWe for a geothermal-BECCS plant (Configuration 2) and 7.8 MWe for a geothermal-DACCS plant (Configuration 3). With a geogenic emissions intensity of 75 gCO_2/kWh, all configurations vent 8.1 $ktCO_2$/year from the cooling tower. The geothermal-BECCs design, which sources 25.4 kt/year of forestry residues for biomass boosting, would also incur 0.21 tCO_2/year of transport emissions for feedstock at 80 km distance.

Table 6: Techno-economic model results for all configurations (100 kg/s of geothermal fluid, CO_2 price = \$100/tonne, feedstock price = \$88/tonne, electricity price = \$60/MWh)

	Base Geothermal (Config. 1)	**Geothermal-BECCS (Config. 2)**	**Geothermal-DACCS (Config. 3)**
Geogenic emissions ($ktCO_2$/year)	8.1	8.1	8.1
Transport emission ($ktCO_2$/year)	0	0.21	0

Biomass burn rate (kt/year)	0	25.4	0
Gross sequestration ($ktCO_2$/year)	0	40.6	49.1
Net emissions ($ktCO_2$/year)	8.1	-32.3	-41.0
Plant capacity (MWe)	13.7	16.5	7.8
EI (gCO_2/kWh)	75	-248	-663
Total CAPEX ($M)	65.6	80.4	103
LCOE ($/MWh)	81	69	143
LCOS ($/$tCO_2$)	-	137	225
LCCA ($/$tCO_2$)	249	145	197

Geothermal-BECCS and geothermal-DACCS with CDR achieve net negative emissions of 32.3 and 41.0 $ktCO_2$/year. Assuming a capacity factor of 90%, the corresponding emission intensities are -248 and -663 gCO_2/kWh, respectively. For reference, the respective positive emission intensities of coal and natural gas generation are about 400 and 1000 gCO_2/kWh (EIA, 2021). We note that neither geothermal-BECCS nor geothermal-DACCS plant could sequester emissions at the same rate as standalone BECCS configuration (e.g., Khallaghi et al., 2021; Yang et al., 2021, see Table 3). This reflects a fundamental limit of dissolving CO_2 in brine when compared to conventional CCS that can inject a pure CO_2 fluid.

In terms of total CAPEX, the base geothermal plant was the cheapest at $65.6 million. The addition of the biomass boiler, ASU and CPU increased the CAPEX of geothermal-BECCS to $80.4 million. Finally, although geothermal-DACCS omitted CAPEX costs from a binary cycle, total CAPEX was nevertheless higher at $103 million due to the substantial cost of DACCS units ($788.4/$tCO_2$, Fahisi et al., 2019; Roestenberg, 2015).

For reference price assumptions (Table 5), geothermal-BECCS had the lowest LCOE (69 $/MWh; Table 6). Although costs of geothermal-BECCS exceed the base geothermal design, the inclusion of CDR revenue lowers the overall LCOE of the plant (Fig. 5A).

When divided into cost components, the CAPEX component of base geothermal ($58.8/MWh) was similar to geothermal-BECCS ($59.7/MWh). However, the OPEX component was higher for geothermal-BECCS ($14.8/MWh and $17.6/MWh, respectively.)

Net emissions to the atmosphere for the base geothermal case are also a cost, contributing $7.5/MWh to total LCOE ($81/MWh). In contrast, for geothermal-BECCS, a substantial fuel cost of $17.4/MWh is incurred. Despite this, when CDR revenue of $25/MWh is deducted, the final LCOE is $69/MWh, about 15% lower than the base geothermal case.

Because the geothermal-DACCS plant diverts energy to CDR operations, there is a considerable drop in plant nameplate capacity (7.8 MWe, compared to 13.7 MWe for base geothermal). As an electricity generating enterprise, geothermal-DACCS therefore has a higher final LCOE of $143/MWh. Without the CDR revenue component of $66/MWh, the plant would have an LCOE of $210/MWh.

The financial performance of all three configurations is tied to the market price of CO_2, which is a cost for base geothermal and a revenue when CDR is included. Thus, the sensitivity of LCOE to the CO_2 price, varying from $0 to $200/t$CO_2$, was investigated (Fig. 6A). LCOEs for both geothermal-BECCS and -DACCS decrease as CDR revenues are maximized at higher carbon prices. Geothermal-BECCS produces the lowest cost electricity of the two options across the range tested.

The LCOE of base geothermal trends upwards as CO_2 price increases and becomes more expensive than geothermal-BECCS above ~$65/tonne. Thus, at a price point of $65/t$CO_2$, CDR is a financial incentive for geothermal electricity production. If biomass were unavailable to pursue a geothermal-BECCS design, then CDR through geothermal-DACCS would only be incentivised at ~$180/$CO_2$.

Geothermal-BECCS is different from the other configurations in that its LCOE is also sensitive to the price of available feedstock. When tested across a range of $0-200/tonne of feedstock (Fig. 6B), geothermal-BECCS is cheaper than base geothermal below a price point of ~$145/tonne. If feedstock were available at zero cost, geothermal-BECCS would have an LCOE of ~$51/MWh.

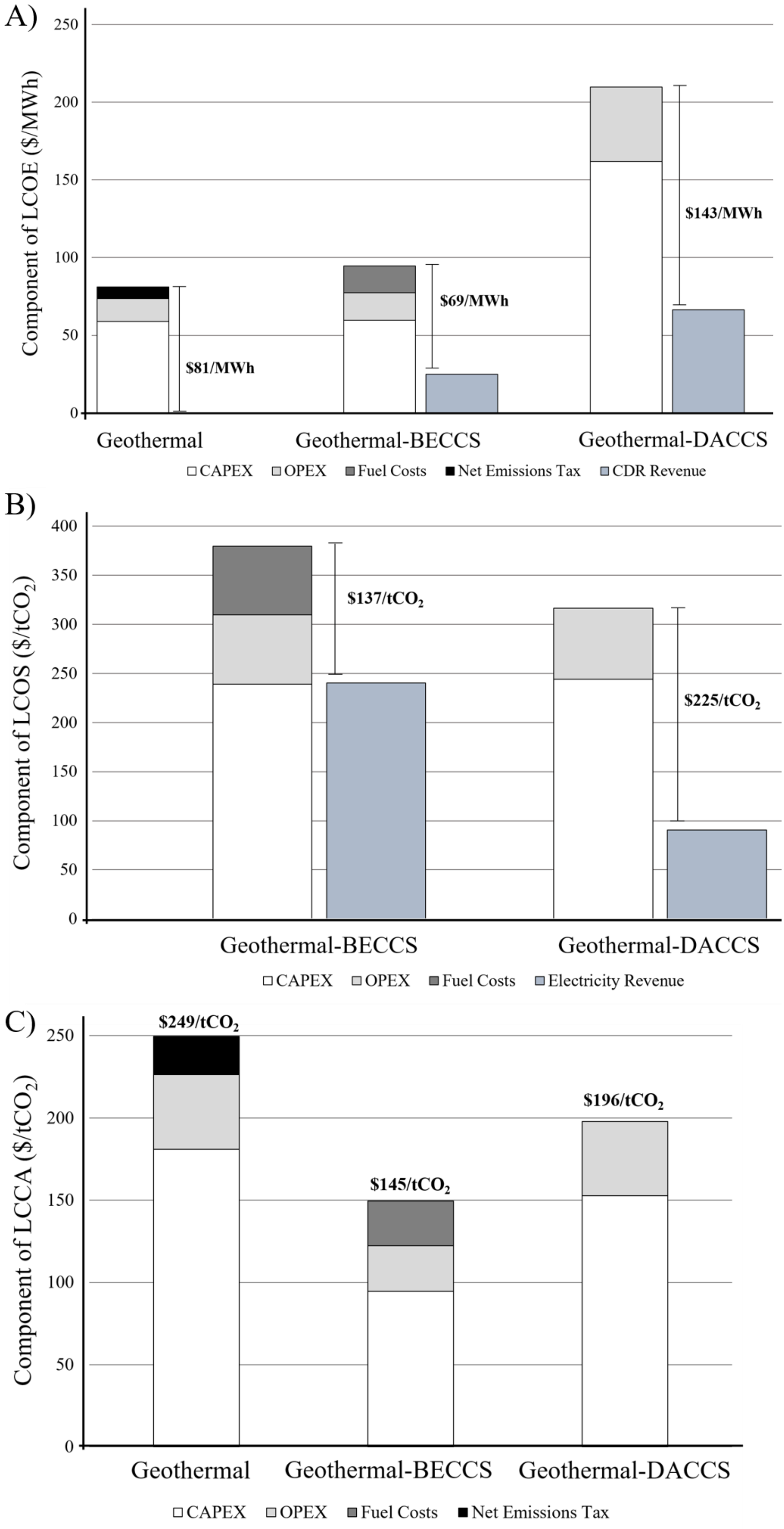
A)
Component of LCOE ($/MWh)
0
50
100
150
200
250
$81/MWh
$69/MWh
$143/MWh
Geothermal
Geothermal-BECCS
Geothermal-DACCS
CAPEX
OPEX
Fuel Costs
Net Emissions Tax
CDR Revenue
B)
Component of LCOS ($/tCO2)
0
50
100
150
200
250
300
350
400
$137/tCO2
$225/tCO2
Geothermal-BECCS
Geothermal-DACCS
CAPEX
OPEX
Fuel Costs
Electricity Revenue
C)
Component of LCCA ($/tCO2)
0
50
100
150
200
250
$249/tCO2
$145/tCO2
$196/tCO2
Geothermal
Geothermal-BECCS
Geothermal-DACCS
CAPEX
OPEX
Fuel Costs
Net Emissions Tax

Figure 5: (A) Electricity cost and CDR revenue component analysis of LCOE for the three geothermal plant designs, (B) CDR cost and electricity revenue component analysis for LCOS for the two geothermal carbon removal designs, and (C) carbon abatement cost component analysis for LCCA for the three geothermal plant designs.

In certain circumstances, carbon removal may take priority over electricity generation (Bistline & Blanford, 2021). In this case, the cheapest form of CDR would be preferred over the cheapest production of electricity – this is quantified via LCOS.

At an electricity price of \$60/MWh, geothermal-BECCS had a lower sequestration cost than geothermal-DACCS. An important caveat, however, is that geothermal-BECCS had higher overall cost components (Fig. 5B) and only achieves a lower LCOS through revenue offsets. At \$260/tCO_2, the electricity revenue for geothermal-BECCS is much higher than the \$96/tCO_2 for geothermal-DACCS. This is because a BECCS process increases available energy for electricity generation whereas the parasitic loads of a DACCS process reduces it.

The enhanced electricity generation revenue largely offsets the LCOS fuel cost component for geothermal-BECCS (\$74/tCO_2). This was the key factor in its performance as both geothermal-BECCS and geothermal-DACCS had otherwise very similar CAPEX (\$259/tCO_2 & \$251/tCO_2) and OPEX (\$76/tCO_2 & \$74/tCO_2) components of LCOS. Importantly, this suggests that geothermal-BECCS is below the \$200/tCO_2 threshold from Sabatino et al. (2021) used to classify uneconomic CDR projects. Although geothermal-DACCS is slightly above the threshold, it remains competitive when compared to LT-DACCS (Lehtveer & Emanuelsson, 2021).

The financial performance of both geothermal carbon removal configurations is sensitive to the price of electricity (Fig. 6C). Geothermal-BECCS sits below the uneconomic threshold of \$200/tCO_2 of electricity prices above \$45/MWh, while geothermal-DACCS only drops below when electricity prices exceed ~\$75/MWh.

At an electricity price of ~\$90/MWh, there is no effective cost to doing CDR through geothermal-BECCS. This is significant because flexible biomass hybridisation could allow some geothermal-BECCS configurations to respond to peak demand periods, accessing higher electricity prices. During these periods, concurrent CDR activities could be very cost-efficient.

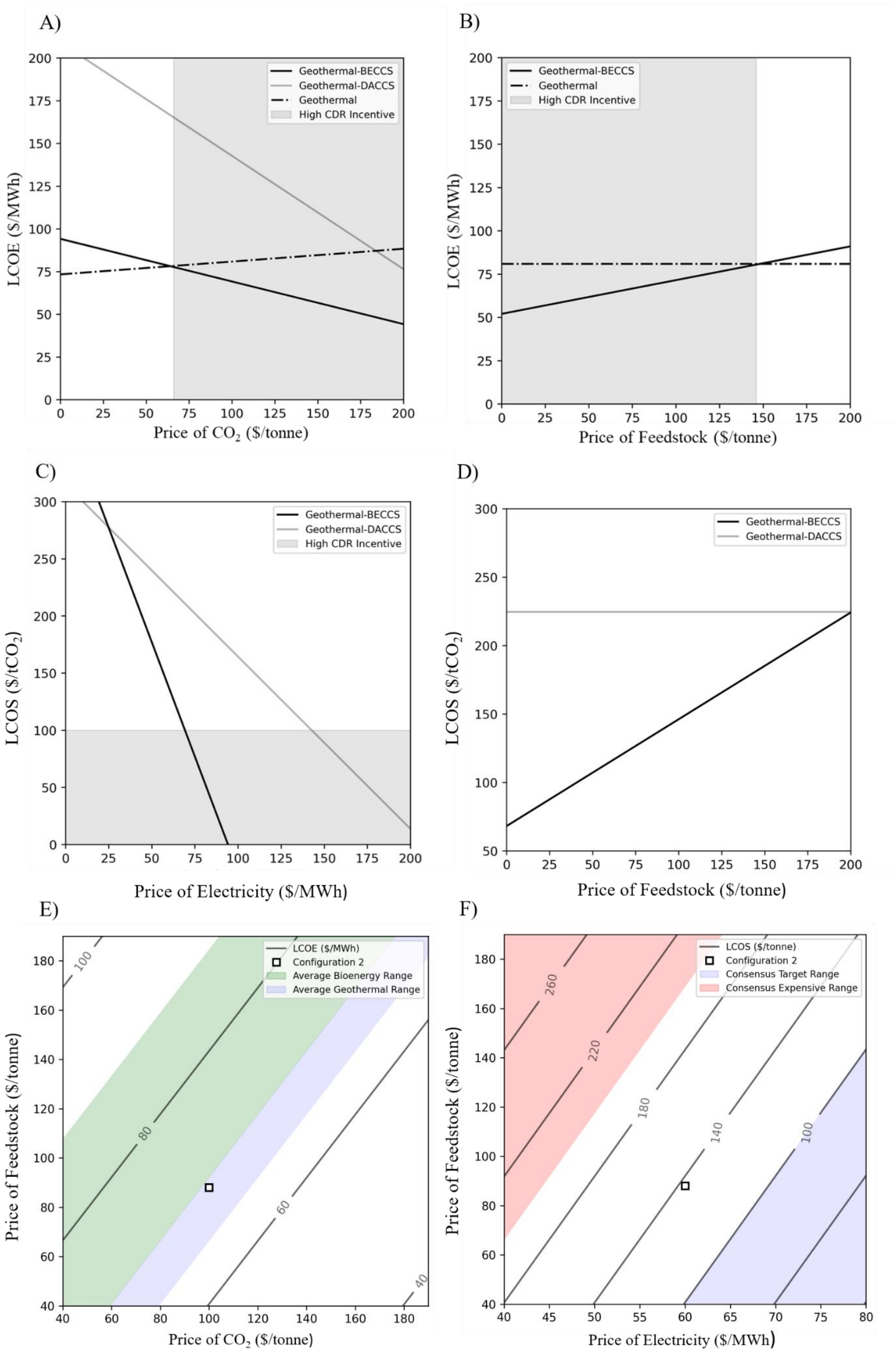

A)
Geothermal-BECCS
Geothermal-DACCS
Geothermal
High CDR Incentive
LCOE ($/MWh)
Price of CO2 ($/tonne)
B)
Geothermal-BECCS
Geothermal
High CDR Incentive
LCOE ($/MWh)
Price of Feedstock ($/tonne)
C)
Geothermal-BECCS
Geothermal-DACCS
High CDR Incentive
LCOS ($/tCO2)
Price of Electricity ($/MWh)
D)
Geothermal-BECCS
Geothermal-DACCS
LCOS ($/tCO2)
Price of Feedstock ($/tonne)
E)
LCOE ($/MWh)
Configuration 2
Average Bioenergy Range
Average Geothermal Range
100
80
60
40
Price of Feedstock ($/tonne)
Price of CO2 ($/tonne)
F)
LCOS ($/tonne)
Configuration 2
Consensus Target Range
Consensus Expensive Range
260
220
180
140
100
Price of Feedstock ($/tonne)
Price of Electricity ($/MWh)

Figure 6: Sensitivity analysis of (A) the market price of CO_2 on LCOE for all three geothermal configurations, (B) the market price of forestry residues on LCOE for all three geothermal configurations, (C) the market price of electricity on LCOS for geothermal carbon removal designs, (D) the market price of forestry residues on LCOS for geothermal carbon removal designs, (E) the sensitivity of LCOE to feedstock and CO_2 price for geothermal-BECCS and (F) and sensitivity of LCOS to feedstock and electricity price for Geothermal-BECCS. For Figure 6E and 6F, Performance under reference price settings is shown by the open square.

Sequestration costs for geothermal-BECCS are sensitive to the market price of forestry residues. We tested a range of feedstock prices from $0 to 200/tonne of feedstock. If feedstock is acquired at zero-cost, the LCOS for geothermal-BECCS is ~$74/t$CO_2$ (Fig. 6D). Every $10/tonne increase in feedstock price results in a ~$7.5/t$CO_2$ increase. Geothermal-BECCS and DACCS have similar costs ($225/t$CO_2$) at a feedstock price of $200/tonne.

Fig. 6E and 6F shows how the LCOE and LCOS of geothermal-BECCS covary across a range of feedstock, CO_2 and electricity prices. With each black line as a contour for LCOE (Fig. 6E) and LCOS (Fig. 6F), it is easier to determine what prices allow for competitive electricity generation and CDR. For example, at a feedstock price of $100/tonne, a competitive LCOE of $60/MWh is only achieved when the CO_2 price exceeds ~$145/tonne.

At the reference price conditions (Table 5), the LCOE of geothermal-BECCS sits below the weighted average LCOE range for bioenergy plants and within the weighted average for geothermal plants (IRENA, 2021). It is also nearer the LCOS targeted range of $100/t$CO_2$ than the consensus uneconomic threshold of $200/t$CO_2$ (Sabatino et al., 2021).

Due to integrated CDR activities, both geothermal-BECCS and DACCS are more effective at displacing fossil emissions (LCCA of $145/$CO_2$ and $197/$CO_2$, respectively) compared to a base geothermal plant (LCCA of $249/$CO_2$; see Fig. 5C). Geothermal-BECCS owes its higher cost competitiveness to comparatively lower CAPEX and OPEX contributions, $95/t$CO_2$ and $28/t$CO_2$, respectively (about half the values for base geothermal, $181/t$CO_2$ and $46/t$CO_2$). The LCCA fuel cost component for geothermal-BECCS ($27/t$CO_2$) was only slightly higher than the geogenic emissions cost of base geothermal ($23/t$CO_2$).

For geothermal-BECCS, we found that feedstock price was not prohibitive to LCCA. At a feedstock price of $200/tonne, the LCCA is $179/t$CO_2$, which is still a more effective decarbonization option than base geothermal or geothermal-DACCS. Every $10/tonne decrease in feedstock price results in a decrease in LCCA of $3/t$CO_2$. If feedstock was acquired at zero cost, the LCCA of geothermal-BECCS would be $119/t$CO_2$.

3.3 Effect of geogenic CO_2 presence on geothermal-CDR performance

Consideration of the geogenic emissions context is important. For geothermal systems with high concentrations of CO_2 being brought up in the geothermal fluid, it is possible for geothermal-BECCS and geothermal-DACCS to no longer facilitate negative emissions. For example, geothermal systems in Türkiye tend to have EIs rivalling coal power plants (Aksoy, 2014).

We calculated net emission intensities for both geothermal-BECCS and geothermal-DACCS across a range of base EI values from 0 to 1000 gCO_2/kWh (Fig. 7A). Net negative emissions are only maintained when the base EI is below ~400 and ~450 gCO_2/kWh for geothermal-BECCS and geothermal-DACCS, respectively.

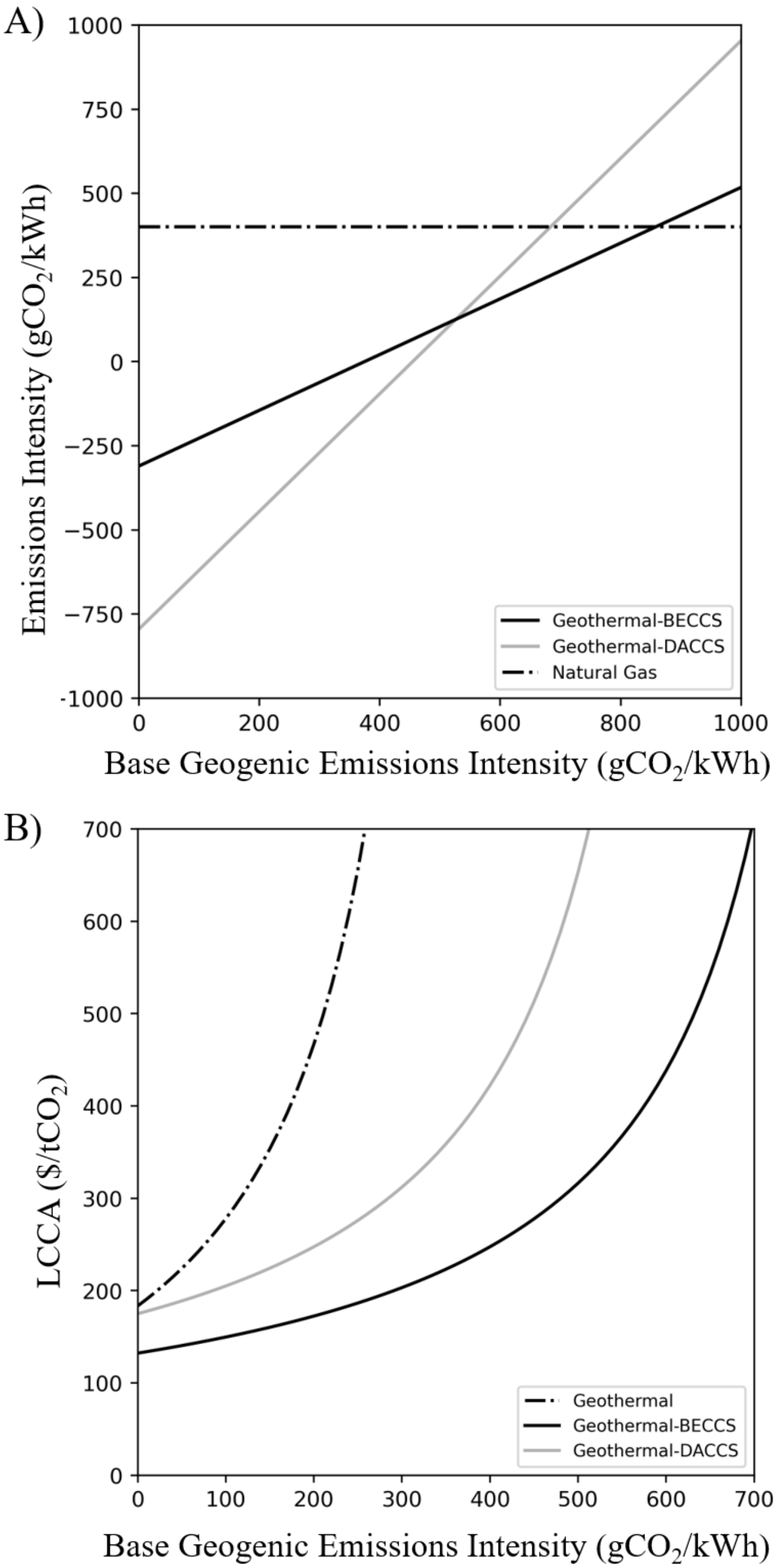

Figure 7: Sensitivity analysis of the base field's geogenic emissions on (A) net EI and (B) on LCCA for geothermal carbon removal designs.

At higher base geothermal emissions, beyond 675 and 875 gCO_2/kWh, respectively, neither geothermal-BECCS or geothermal-DACCS can effectively displace emissions from natural gas. These values are much higher than the world wide average EI of geothermal fields at 122 gCO_2/kWh (Bertani & Thain, 2002), but lower than the average EI of fields in Türkiye (1000 gCO_2/kWh).

LCCA is also sensitive to the base geogenic EI of the geothermal system. LCCA considers the displacement effect of CO_2 in the system (Eq. 4), geothermal systems with inherently high geogenic emissions are less effective at abating fossil emissions. Presently, an LCCA above \$200/tCO_2 is considered expensive (Friedmann et al., 2020) and indicative of cheaper alternatives for decarbonisation.

The base geothermal plant has an LCCA of \$200/tCO_2 for geogenic CO_2 emissions of ~20 gCO_2/kWh (Fig. 7B). Above this threshold, traditional geothermal generation can be considered an expensive technology for displacing natural gas. Geothermal-DACCS crosses the same cost threshold at a base geogenic CO_2 EI of 100 gCO_2/kWh, which is above the average for New Zealand's geothermal systems, indicating it would be a more cost effective tool for abating natural gas generation.

Geothermal-BECCS is ultimately the most cost-effective of the three configurations at displacing natural gas emissions, only crossing the \$200/tCO_2 threshold for geothermal systems whose geogenic EI exceeds 300 gCO_2/kWh. For systems with geogenic EI exceeding 400 gCO_2/kWh, none of the configurations are cost-effective technologies for displacing emissions from natural gas power plants. This makes both BECCS and DACCS activities potentially unsuitable for geothermal fields with outlier emissions.

4. Discussion

4.1. Opportunities and challenges for geothermal-CDR

Pathways to scalability often use 1 $MtCO_2$/year as an order of magnitude to consider feasibility. For geothermal-BECCS to achieve a CDR at this scale , we would require 3000 kg/s of geothermal fluid supporting a hybrid plant capacity of 512 MWe. Assuming an average geothermal well mass flow rate of 50 kg/s (DiPippo, 2016), this corresponds to about 60 wells. For context, in 2008 New Zealand's Wairakei Power Station with installed capacity of 175 MWe had 59 active production wells (Bixley et al., 2009).

For geothermal-DACCS to achieve the same scale of CDR, approximately 2440 kg/s of geothermal fluid (49 wells) would be needed. Accounting for the parasitic loads of air capture from over 24 000 collectors, the net plant capacity would be 190 MWe. The total investment costs for these plants is similar: \$2.4 billion for geothermal-BECCS and \$2.5 billion for geothermal-DACCS.

A geothermal-BECCS plant sequestering 1 $MtCO_2$/year would require about 790 kt/year of feedstock for the energy content assumed here (16 MJ/kg). For context, New Zealand currently generates 3 Mt/year of forestry residues (MPI, 2020) and California is forecast to generate up to 24 Mt/year of forestry residues by 2025 (Baker et al., 2015). Indeed, California already has a large amount of geothermal with an installed capacity of 2.8 GWe (Tarroja et al., 2018). In a scenario where this was doubled through the construction of new geothermal-BECCS plants, this would induce a 4.3 Mt/year demand for forestry residues (about 18% of forecast resource) and result in net negative emissions of 5.5 $MtCO_2$/year.

In contrast, implementation of geothermal-BECCS is likely to be difficult in Iceland. This is because, with only 2% of the country's land area covered by forests (Pálsdóttir et al., 2022), biomass feedstock is likely to be limited. In this case, and in other locales where biomass is unavailable or expensive, geothermal-DACCS would be the obvious pathway for CDR.

Biomass transport distance has only a minor effect on the emissions performance of geothermal-BECCS plants. Every increase in 100 km biomass transport distance contributes only 2 gCO_2/kWh to total EI. The corollary is that there are only marginal emissions benefits from developing on-site feedstock options and factors other than transport should be prioritised when considering biomass supply, e.g., harvest practices, feedstock calorific properties.

In contrast, base geogenic emissions could be a major constraint on the decision to decarbonize individual geothermal sites, with values in Türkiye (~1000 gCO_2/kWh) being prohibitively higher than the threshold for negative emissions to no longer be achievable for geothermal-BECCS and geothermal-DACCS (geogenic EI of ~400 gCO_2/kWh and ~450 gCO_2/kWh, respectively.

4.2. The importance of boiler capital investment cost reduction

CAPEX rates for bioenergy tend to be higher in North America and Europe than in China and India (IRENA, 2021). This is significant for geothermal-BECCS because the latter nations have less abundant geothermal resources. It suggests a potential nation-level mismatch between geothermal opportunity and the economic means to exploit using bioenergy.

As an example, the bioenergy plant with the highest CAPEX rate in 2021 was a European plant that used wood waste products. It had a CAPEX rate of \$7694/kWe, which is over three times the global average (IRENA, 2021). If this high value was used for the geothermal-BECCS design investigated here, total CAPEX increases to \$109 million. Accordingly, LCOE, LCOS and LCCA increase to \$102/MWh, \$267/tCO_2 and \$195/tCO_2, respectively. Although LCOE and LCCA are still favourable compared to geothermal-DACCS (\$143/MWh, \$197/tCO_2), the LCOS is now \$42/tCO_2 more expensive (\$225/tCO_2).

This sensitivity analysis also illustrates a counterintuitive property of the different financial performance metrics. Although the geothermal-BECCS plant with high CAPEX described above produces higher cost electricity than the base geothermal plant (\$81/MWh), it is still the cheaper option for emissions abatement with an LCCA below that of base geothermal (\$249/tCO_2). That is, compared to conventional geothermal, geothermal-BECCS is simultaneously \$21/MWh more expensive for generating electricity but \$54/tCO_2 cheaper for abating natural gas emissions. Thus, with a discernible opportunity cost between the two plants, the configuration selected would depend on the contextual priorities surrounding that geothermal system.

4.3. Retrofit of existing geothermal plants

A major cost component of geothermal-BECCS is the high upfront capital embodied in turbines, the above-ground pipe network, and well infrastructure. Rather than investing this infrastructure from scratch, a lower cost option could be to retrofit an existing geothermal plant that has already paid off these components. Although a practical retrofit design would need to be tailored to the specifics of the original plant, we can obtain an initial cost estimate through a modification of the LCCA calculation (Eqn. 6):

$$LCCA_{Retrofit} = \frac{C_1' - C_0'}{E_0' - E_1'} \tag{6}$$

where C_1' is the generation-levelized cost for geothermal-BECCS (all CAPEX, OPEX & fuel costs) in \$/MWh, C_0' is the generation-levelized cost of the original geothermal plant (geothermal infrastructure CAPEX, geothermal OPEX & net tax for geogenic emissions), E_1' is the generation-levelized emissions of the geothermal-BECCS plant (net negative, accounting for geogenic emissions offset) in $kgCO_2$/MWh, and E_0' is the generation-levelized emissions of the original geothermal plant. Because the two plants have different nameplate capacities, a fair comparison can only be made on a per unit of generated electricity basis. Hence, we have used cost and emissions terms scaled by net generation from the associated plant, i.e., $E_1' = E_1/G_1$ where G_1 is the net electricity generated by the geothermal-BECCS plant in MWh. All terms are discounted over the plant lifetime.

This formulation of LCCA is different compared to Eqn. (5) through the inclusion of the term $C_0{}'$. Eqn. (5) assumes that costs of the natural gas plant BAU are not incurred by the geothermal plant owner and therefore should not be considered. However, for a retrofit the geothermal plant owner incurs costs from the BAU and the new configuration. Therefore, any costs avoided, such as future geogenic emissions or existing capital, should be deducted.

For this retrofit example, we consider the benchmark geothermal plant (configuration 1, 13.7 MWe) being reconfigured into a geothermal-BECCS plant (configuration 2, 16.5 MWe). Generation-levelized cost (C_0') of the geothermal plant is \$81/MWh and this is deducted from the equivalent geothermal-BECCS cost (C_1') of \$94/MWh. The emissions intensities of the two plants are 75 and -248 $kgCO_2$/MWh, respectively. Hence, the LCCA for retrofit is \$41 for each tonne of CO_2 abated under reference market conditions (Table 5). This is substantially lower than the \$145/tCO_2 for a greenfield geothermal-BECCS plant (Fig. 5C) and highlights the major advantage of retrofitting existing geothermal developments.

Because the cost of net positive CO_2 emissions is factored into C_0', changes to the market price of CO_2 will affect LCCA. The lower the market price of CO_2, the less incentive there would be to abate geothermal with geothermal-BECCS. However, even at a CO_2 price of \$0/tCO_2, we found that the retrofit LCCA only increased to \$64 per tonne of CO_2 abated.

Retrofit LCCA varies linearly with the fuel price and drops to -\$12/tCO_2 if forestry residues can be sourced at zero cost. This is because the total costs per generation term of the retrofit plant reduces to \$77/MWh while continuing to generate more electricity at a constant mass production rate (100 kg/s). In this case, it would save \$12 in costs to abate each tonne of CO_2 by retrofitting a conventional geothermal plant to geothermal-BECCS. Again, we emphasize that use of existing geothermal infrastructure and sourcing low cost biomass feedstocks are key to cost effective decarbonisation via geothermal-BECCS.

Given the improved performance, a global inventory of retrofit potential for geothermal-CDR systems that characterizes electricity generation, annual CDR potential and feedstock availability could be valuable next step in supplementing decarbonisation initiatives in accordance with AR6. However, careful consideration would need to be given to reservoir management that minimizes CO_2 breakthrough and any additional potential for corrosion of plant or wellfield assets.

4.4. Assessing geothermal-CDR as a decarbonisation tool

In terms of overall decarbonisation, we found that the displacement effect of negative emissions from geothermal-CDR is far stronger than the lower carbon emissions from conventional geothermal (> 0 gCO_2/kWh), even when there is less renewable electricity produced in the case of geothermal-DACCS.

Geothermal-BECCS is advantaged over conventional geothermal and geothermal-DACCS because of the net increase in electricity production, but requires a reliable source of feedstock. The role of bioenergy in climate change mitigation is not without concerns (Sandalow et al., 2020), namely competition with food production for land use and supply chain uncertainties.

Geothermal-DACCS side-steps this risk and sequesters more CO_2 per rate of electricity generated. However, to reach equivalent generation for a given resource temperature, geothermal-DACCS requires higher fluid extraction from and reinjection into the system. These activities are not without environmental impacts, such as subsidence due to local depressurization (Allis, 2000) or induced seismicity around reinjection wells (Majer & Peterson, 2007). Although these are challenges for any geothermal development, they will be exacerbated wherever plant design imposes a higher physical load on the geothermal system.

For geothermal-DACCS, the separated brine must be delivered at temperatures ~100°C. This depends in turn on both the reservoir temperature that the geofluid is sourced from as well as the condenser temperature (DiPippo, 2016). For the condenser used in this study (43.85°C), the minimum reservoir temperature that can be used to produce separated brine at 100°C is 153°C. The efficiency of geothermal power plants typically declines with reservoir temperature, thus the parasitic load of DACCS will grow proportionally for lower temperature systems (<160°C). Thus, if provision of low-emissions electricity is priority, geothermal-BECCS may be better suited to lower temperature resources due to the additional boosting.

However, electricity provision may not be a priority in all contexts. In certain circumstances, the CDR value of a given biomass feedstock could outweigh its electricity value, a concept known as the Aines Principle (Sandalow et al., 2020). Thus, geothermal-BECCS cycles that produce biochar or biohydrogen (through oxy-gasification) could be valuable to explore in markets where electricity generation is highly competitive. In theory, a geothermal-BECCS cycle that co-produces electricity, heat, biohydrogen and CDR is possible, but its economic feasibility will depend on site-specific conditions and market demands for those outputs.

Optimization between cost effective electricity generation and CDR are difficult decisions to make when choosing between decarbonisation initiatives. Importantly, the key metrics used in this study (LCOE, LCOS, LCCA & EI) are best considered collectively because no single one quantifies the whole picture. For example, LCOE does not recognize overall CO_2 reduction in the system (Friedmann et al., 2020) and so has limited utility when informing decarbonisation policy. In contrast, demands from a dynamic electricity market, with daily and seasonal fluctuations in demand, are not captured in either LCOS or LCCA (Lehtveer & Emanuelsson, 2021). Additionally, CDR activities may be incentivised only in periods when electricity prices are high.

LCCA may be best suited to governments or organizations concerned with decarbonizing their activities through technology switching. Thus, selecting the original emitter or 'business as usual' case becomes critical to the analysis. For example, if the three configurations considered here were used to instead displace an equivalent-sized coal plant (1000 gCO_2/kWh), the denominator in Eqn. 4 would be significantly larger and the three configurations would all appear more cost-effective.

Unlike LCCA, the EI doesn't capture the efficacy of potential CO_2 displaced by increased renewable power in the overall energy system. For example, geothermal-BECCS removes 20% less CO_2 than geothermal-DACCS but it produces over two times the low-emissions electricity. The CO_2 displacement effect of the increased electricity is not reflected in the EI metric. This could be distorting in settings where affordable low-emissions electricity is a more valuable resource than CDR.

All CDR technologies are subject to social, policy and market framework challenges (Gough et al., 2018). Robust policy targets, akin to those of solar-PV development from 1996-2005, will be critical if CDR is to be implemented at scale (Breyer et al., 2019). Lowering CAPEX rates for both geothermal-BECCS and geothermal-DACCS should be a key endeavour when pursuing CDR opportunities in geothermal systems, as CAPEX has the highest weighting by component across LCOE, LCOS and LCCA for both geothermal-BECCS and geothermal-DACCS. Finally, negative emissions technologies must be deployed in conjunction with, and not in lieu of, conventional emissions reduction methods.

5. Conclusion

Geothermal energy has the potential for cost-competitive direct and biogenic carbon dioxide removal. Using in-line dissolution of emissions in reinjection wells, geothermal combined either with BECCS or DACCS becomes a technology for meeting both low-emissions electricity and CDR targets as required in IPCC pathways for climate change mitigation. Here, we quantified these processes for a hypothetical geothermal system with adjacent forestry resources.

We considered a reference plant configuration based on 100 kg/s of geothermal fluid obtained from a reservoir at 275°C, and within 80 km of a forestry biomass source. Our results showed that a conventional geothermal plant would produce 13.7 MWe with natural geogenic emissions of 8.1 ktCO_2/year. In contrast, when integrated with bioenergy and emissions capture, a geothermal-BECCS plant would have 20% higher electricity production (16.5 MWe) and atmospheric emissions removal of 32.3 ktCO_2/year. By comparison, parasitic loads mean that a geothermal-DACCS plant generates 43% less net electricity (7.8 MWe) although with a higher emissions removal rate of 41.0 ktCO_2/year. Accordingly, geothermal-DACCS has the highest negative emissions intensity (-663 gCO_2/kWh) followed by geothermal-BECCS (-248 gCO_2/kWh).

At reference market prices of CO_2 ($100/tonne), forestry residues ($88/tonne) and electricity ($60/MWh), geothermal-BECCS has the lowest levelized costs of electricity (LCOE, $69/MWh), sequestration (LCOS, $137/t$CO_2$) and carbon abatement (LCCA, $145/t$CO_2$). Although a base geothermal plant is a more effective design than geothermal-DACCS for generating low-emission electricity (LCOE of $81/MWh vs $143/MWh), it is less effective technology for abating total emissions (LCCA of $249/t$CO_2$ vs. $197/$CO_2$) using natural gas generation as a reference. CAPEX was the dominant contributor to costs across all three plant designs. LCCA is improved further when considering a retrofit pathway for geothermal-BECCS with a conventional geothermal plant as the reference. CAPEX cost reductions from leveraging existing infrastructure (plant, pipes, wells) drop the LCCA to $41/t$CO_2$.

Both geothermal-BECCS and geothermal-DACCS could achieve CDR rates of 1 MtCO_2/year at investment costs of $2.4 billion (512 MWe, 788 kt/year of forestry residues) and $2.5 billion (190 MWe), respectively. This could be met with the same number of production wells already available at, for example, the Wairakei Power Station in New Zealand.

Geothermal-DACCS requires no fuel source but may be limited by sufficient geothermal resource temperature. Successful deployment in the future will depend on minimizing parasitic loads and capture infrastructure costs through technological improvement. Geothermal-BECCS could theoretically be applied to lower temperature geothermal systems but requires suitable and available feedstocks and reductions in boiler capital costs. There may be scope for ancillary biohydrogen production to compliment electricity generation, a prospect that warrants further investigation.

We showed that under the right market incentives, geothermal based CDR schemes can be financially viable and strategically valuable by offering dual decarbonisation through grid emissions displacement and residual CO_2 abatement at similar costs to conventional geothermal power plants. CDR. Furthermore, cost effective CDR in the near term from geothermal-BECCS and geothermal-DACCS will require the refurbishment of existing geothermal infrastructure. We conclude that the increase in electricity production for geothermal-BECCS makes it more cost-effective than geothermal-DACCS at the reference market conditions of this study.

References

Addison, S. J., Winick, J. A., Sewell, S. M., Buscarlet, E., Hernandez, D., & Siega, F. L. (2015). Geochemical response of the Rotokawa reservoir to the first 5 years of Nga Awa Purua production. In Proceedings 37th New Zealand Geothermal Workshop (Vol. 18, p. 20).

Aksoy, N. (2014). Power generation from geothermal resources in Turkey. Renewable Energy, 68, 595-601.

Allis, R. G. (2000). Review of subsidence at Wairakei field, New Zealand. Geothermics, 29(4-5), 455-478.

Allis, R., Moore, J., Blackett, B., Gwynn, M., Kirby, S., & Sprinkel, D. (2011). The potential for basin-centered geothermal resources in the Great Basin. Geothermal Resources Council Transactions, 35, 683-688.

Anno, G. H., Dore, M. A., Grijalva, R. L., Lang, G. D., & Thomas, F. J. (1977). Site-specific analysis of hybrid geothermal/fossil power plants (No. PSR-705). Pacific Sierra Research Corp., Santa Monica, Calif.(USA).

Baker, S. E., Stolaroff, J. K., Peridas, G., Pang, S. H., Goldstein, H. M., Lucci, F. R., ... & McCormick, C. (2020). Getting to neutral: options for negative carbon emissions in California (No. LLNL-TR-796100). Lawrence Livermore National Lab.(LLNL), Livermore, CA (United States); Univ. of California, Berkeley, CA (United States); Negative Carbon Consulting, Half Moon Bay, CA (United States); Univ. of Calgary, AB (Canada); Univ. of Queensland, Brisbane, QLD (Australia); Univ. of California, Davis, CA (United States); Worcester Polytechnic Institute, MA (United States); Georgetown Univ., Washington, DC (United States); Valence Strategic, Washington, DC (United States).

Bayer, P., Rybach, L., Blum, P., & Brauchler, R. (2013). Review on life cycle environmental effects of geothermal power generation. Renewable and Sustainable Energy Reviews, 26, 446-463.

Bertani, R., & Thain, I. (2002). Geothermal power generating plant CO2 emission survey. IGA news, 49, 1-3.

Bistline, J. E., & Blanford, G. J. (2021). Impact of carbon dioxide removal technologies on deep decarbonization of the electric power sector. Nature Communications, 12(1), 3732.

Bixley, P. F., Clotworthy, A. W., & Mannington, W. I. (2009). Evolution of the Wairakei geothermal reservoir during 50 years of production. Geothermics, 38(1), 145-154.

Bonafin, J., Pietra, C., Bonzanini, A., & Bombarda, P. (2019). CO2 emissions from geothermal power plants: evaluation of technical solutions for CO2 reinjection. In Proceedings of the European Geothermal Congress.

Boseley, C., Cumming, W., Urzúa-Monsalve, L., Powell, T., & Grant, M. (2010). A resource conceptual model for the Ngatamariki geothermal field based on recent exploration well drilling and 3D MT resistivity imaging. In Proceedings world geothermal congress

Breyer, Christian, Mahdi Fasihi, Cyril Bajamundi, and Felix Creutzig (2019). "Direct air capture of CO2: a key technology for ambitious climate change mitigation." Joule 3, no. 9: 2053-2057.

Cheng, F., Small, A. A., & Colosi, L. M. (2021). The levelized cost of negative CO2 emissions from thermochemical conversion of biomass coupled with carbon capture and storage. Energy Conversion and Management, 237, 114115.

Dal Porto, F., Pasqui, G., & Fedeli, M. (2016). Geothermal power plant production boosting by biomass combustion: Cornia 2 case study. Proceedings of the European Geothermal Congress,

Dickson, M. H., & Fanelli, M. (2013). Geothermal energy: utilization and technology. Routledge.

Dinca, C., Slavu, N., Cormoş, C. C., & Badea, A. (2018). CO2 capture from syngas generated by a biomass gasification power plant with chemical absorption process. Energy, 149, 925-936.

DiPippo, R. (2016). Geothermal Power Plants: Principles, Applications, Case Studies and Environmental Impact 4th ed., Elsevier Science.

Duan, Z., & Sun, R. (2003). An improved model calculating CO2 solubility in pure water and aqueous NaCl solutions from 273 to 533 K and from 0 to 2000 bar. Chemical Geology, 193(3-4), 257-271.

EIA. (2021). Annual Energy Outlook 2021. https://www.eia.gov/outlooks/aeo/

Emenike, O., Michailos, S., Finney, K. N., Hughes, K. J., Ingham, D., & Pourkashanian, M. (2020). Initial techno-economic screening of BECCS technologies in power generation for a range of biomass feedstock. Sustainable Energy Technologies and Assessments, 40, 100743.

Fasihi, M., Efimova, O., & Breyer, C. (2019). Techno-economic assessment of CO2 direct air capture plants. Journal of cleaner production, 224, 957-980.

Friedmann, J., Fan, Z., Byrum, Z., Ochu, E., Bhardwaj, A., & Sheerazi, H. (2020). Levelized cost of carbon abatement: An improved cost-assessment methodology for a net-zero emissions world. Columbia University SIPA Center on Global Energy Policy: New York, NY, USA.

Galiègue, X., & Laude, A. (2017). Combining Geothermal Energy and CCS: From the Transformation to the Reconfiguration of a Socio-Technical Regime? Energy Procedia, 114, 7528-7539.

Garcia, J. E. (2001). Density of aqueous solutions of CO2 (No. LBNL-49023). Lawrence Berkeley National Lab.(LBNL), Berkeley, CA (United States).

García-Luna, S., Ortiz, C., Carro, A., Chacartegui, R., & Pérez-Maqueda, L. A. (2022). Oxygen production routes assessment for oxy-fuel combustion. Energy, 254, 124303.

Gunnarsson, I., Aradóttir, E. S., Oelkers, E. H., Clark, D. E., Arnarson, M. Þ., Sigfússon, B., Snæbjörnsdóttir, S. Ó., Matter, J. M., Stute, M., & Júlíusson, B. M. (2018). The rapid and cost-effective capture and subsurface mineral storage of carbon and sulfur at the CarbFix2 site. International Journal of Greenhouse Gas Control, 79, 117-126.

Gutknecht, V., Snæbjörnsdóttir, S. Ó., Sigfússon, B., Aradóttir, E. S., & Charles, L. (2018). Creating a carbon dioxide removal solution by combining rapid mineralization of CO2 with direct air capture. Energy Procedia, 146, 129-134.

Hanak, D. P., Powell, D., & Manovic, V. (2017). Techno-economic analysis of oxy-combustion coal-fired power plant with cryogenic oxygen storage. Applied Energy, 191, 193-203.

Intergovernmental Panel on Climate Change (IPCC). (2023). Synthesis Report of the IPCC Sixth Assessment Report (AR6): Summary for Policymakers.

IRENA (2019). Renewable Capacity Statistics 2019. International Renewable Energy Agency, Abu Dhabi. https://www.irena.org/publications/2019/Mar/Renewable-Capacity-Statistics-2019

IRENA (2021), Renewable Power Generation Costs in 2021, International Renewable Energy Agency, Abu Dhabi

Kaya, E., & Zarrouk, S. J. (2017). Reinjection of greenhouse gases into geothermal reservoirs. International Journal of Greenhouse Gas Control, 67, 111-129.

Kervévan, C., Beddelem, M.-H., Galiègue, X., Le Gallo, Y., May, F., O'Neil, K., & Sterpenich, J. (2017). Main results of the CO2-DISSOLVED project: first step toward a future industrial pilot combining geological storage of dissolved CO2 and geothermal heat recovery. Energy Procedia, 114, 4086-4098.

Keith, D. W., Holmes, G., Angelo, D. S., & Heidel, K. (2018). A process for capturing CO2 from the atmosphere. Joule, 2(8), 1573-1594.

Khallaghi, N., Jeswani, H., Hanak, D. P., & Manovic, V. (2021). Techno-economic-environmental assessment of biomass oxy-gasification staged oxy-combustion for negative emission combined heat and power. Applied Thermal Engineering, 196, 117254.

Kiani, A., Jiang, K., & Feron, P. (2020). Techno-economic assessment for CO2 capture from air using a conventional liquid-based absorption process. Frontiers in Energy Research, 8, 92.

Kumar, V. V., Hoadley, A., & Shastri, Y. (2019). Dynamic impact assessment of resource depletion: a case study of natural gas in New Zealand. Sustainable Production and Consumption, 18, 165-178.

Lawrence, M. G., Schäfer, S., Muri, H., Scott, V., Oschlies, A., Vaughan, N. E., ... & Scheffran, J. (2018). Evaluating climate geoengineering proposals in the context of the Paris Agreement temperature goals. Nature communications, 9(1), 3734.

Lehtveer, M., & Emanuelsson, A. (2021). BECCS and DACCS as negative emission providers in an intermittent electricity system: why levelized cost of carbon may be a misleading measure for policy decisions. Frontiers in Climate, 3, 647276.

Lugaizi, I. (2011). Borehole geology and hydrothermal mineralisation of well HE-32, Hellisheidi Geothermal Field, SW-Iceland. United Nations University Geothermal Training Programme.

Majer, E. L., & Peterson, J. E. (2007). The impact of injection on seismicity at The Geysers, California Geothermal Field. International Journal of Rock Mechanics and Mining Sciences, 44(8), 1079-1090.

Marieni, C., Přikryl, J., Aradóttir, E. S., Gunnarsson, I., & Stefánsson, A. (2018). Towards 'green'geothermal energy: Co-mineralization of carbon and sulfur in geothermal reservoirs. *International Journal of Greenhouse Gas Control, 77,* 96-105.

McLean, K., Richardson, I., Quinao, J., Clark, T., & Owens, L. (2020). Greenhouse gas emissions from New Zealand geothermal: power generation and industrial direct use. In Proceedings 42nd New Zealand Geothermal Workshop (Vol. 24, p. 26).

MfE. (2022). Measuring emissions: A guide for organisations: 2022 detailed guide. Wellington: Ministry for the Environment.

MPI. (2020). Wood Fibre Futures Stage: One Report. Ministry of Primary Industries.

Nurek, T., Gendek, A., & Roman, K. (2019). Forest residues as a renewable source of energy: Elemental composition and physical properties. BioResources, 14(1), 6-20.

Pálsdóttir, A. E., Gill, J. A., Alves, J. A., Pálsson, S., Méndez, V., Ewing, H., & Gunnarsson, T. G. (2022). Subarctic afforestation: Effects of forest plantations on ground- nesting birds in lowland Iceland. Journal of Applied Ecology, 59(10), 2456-2467.

Park, S., Langat, A., Lee, K., & Yoon, Y. (2021). Measuring the impact of risk on LCOE (levelized cost of energy) in geothermal technology. Geothermal Energy, 9(1), 27.

Pehl, M., Arvesen, A., Humpenöder, F., Popp, A., Hertwich, E. G., & Luderer, G. (2017). Understanding future emissions from low-carbon power systems by integration of life-cycle assessment and integrated energy modelling. Nature Energy, 2(12), 939-945.

Puettmann, M., Sahoo, K., Wilson, K., & Oneil, E. (2020). Life cycle assessment of biochar produced from forest residues using portable systems. Journal of Cleaner Production, 250, 119564.

Ratouis, T. M., Snæbjörnsdóttir, S. Ó., Voigt, M. J., Sigfússon, B., Gunnarsson, G., Aradóttir, E. S., & Hjörleifsdóttir, V. (2022). Carbfix 2: A transport model of long-term CO2 and H2S injection into basaltic rocks at Hellisheidi, SW-Iceland. International Journal of Greenhouse Gas Control, 114, 103586.

Reynolds, W. C. (1979). Thermodynamic properties in SI: graphs, tables, and computational equations for forty substances. Department of Mechanical Engineering, Stanford University.

Roestenberg, T., 2015. Design Study Report - Antecy Solar Fuels Development. Antecy. Hoevelaken, the Netherlands.

Ruiz, J. A., Juárez, M. C., Morales, M. P., Muñoz, P., & Mendívil, M. A. (2013). Biomass gasification for electricity generation: Review of current technology barriers. Renewable and sustainable energy reviews, 18, 174-183.

Sabatino, F., Grimm, A., Gallucci, F., van Sint Annaland, M., Kramer, G. J., & Gazzani, M. (2021). A comparative energy and costs assessment and optimization for direct air capture technologies. Joule, 5(8), 2047-2076.

Sandalow, D., Aines, R., Friedmann, J., McCormick, C., & Sanchez, D. L. (2021). Biomass Carbon Removal and Storage (BiRCS) Roadmap (No. LLNL-TR-815200). Lawrence Livermore National Lab.(LLNL), Livermore, CA (United States).

Sigfusson, B., Gislason, S. R., Matter, J. M., Stute, M., Gunnlaugsson, E., Gunnarsson, I., ... & Oelkers, E. H. (2015). Solving the carbon-dioxide buoyancy challenge: The design and field testing of a dissolved CO2 injection system. International Journal of Greenhouse Gas Control, 37, 213-219.

Tarroja, B., Chiang, F., AghaKouchak, A., & Samuelsen, S. (2018). Assessing future water resource constraints on thermally based renewable energy resources in California. Applied Energy, 226, 49-60.

Titus, K. A., Dempsey, D. E., & Peer, R. A. M. (2023). Carbon negative geothermal: Theoretical efficiency and sequestration potential of geothermal-BECCS energy cycles. International Journal of Greenhouse Gas Control, 122, 103813.

Thain, I., & DiPippo, R. (2015). Hybrid geothermal-biomass power plants: applications, designs and performance analysis. In Proceedings world geothermal congress, Melbourne, Australia (pp. 19-25).

Toselli, D., Heberle, F., & Brüggemann, D. (2019). Techno-economic analysis of a solid biomass retrofit of an air-cooled ORC geothermal power plant.

Vargas, C. A., Caracciolo, L., & Ball, P. J. (2022). Geothermal energy as a means to decarbonize the energy mix of megacities. Communications Earth & Environment, 3(1), 66.

Yang, B., Wei, Y. M., Liu, L. C., Hou, Y. B., Zhang, K., Yang, L., & Feng, Y. (2021). Life cycle cost assessment of biomass co-firing power plants with CO2 capture and storage considering multiple incentives. Energy Economics, 96, 105173.

Zang, G., Jia, J., Tejasvi, S., Ratner, A., & Lora, E. S. (2018). Techno-economic comparative analysis of Biomass Integrated Gasification Combined Cycles with and without CO2 capture. International Journal of Greenhouse Gas Control, 78, 73-84.

Zhou, C., Shah, K., Song, H., Zanganeh, J., Doroodchi, E., & Moghtaderi, B. (2016). Integration options and economic analysis of an integrated chemical looping air separation process for oxy-fuel combustion. Energy & Fuels, 30(3), 1741-1755.